TRANSFORMING COAL INTO PREMIUM CARBON PRODUCTS: AN OUTLOOK

John M. Andresen[1], Joel L. Morrison[1], Frank Rusinko Jr.[1], John W. Zondlo[2], John Stipanovich[3], John C. Winslow[3] and Harold H. Schobert[1]

[1]The Energy Institute, The Pennsylvania State University, 209 Academic Projects Bldg., University Park, PA 16802
[2] Department of Chemical Engineering, College of Engineering and Mineral Resources, P.O. Box 6102, Morgantown, WV 26506-6102
[3]National Energy Technology Laboratory, U.S. Department of Energy, P. O. Box 10940, Pittsburgh, PA 15236-0940

Introduction

The great abundance of coal in the U.S. carries an inherent potential of introducing benign and affordable premium carbon products to the general public (1). Low cost carbon fibers from coal could ensure lighter vehicles and result in a tremendous rise in energy efficiency for the traffic sector. Large production of inexpensive activated carbon could significantly increase the use of activated carbon in water treatment facilities thus vastly improve water quality throughout US. Further, high quality binder pitches and cokes for anodes in the aluminum industry and electrodes for the steel industry can be derived from coal. An industry driven consortium, Consortium for Premium Carbon Products from Coal, has for the last four years strived for the recognition of coal as a valuable resource for producing premium carbon products and some of its recent advances are discussed.

Carbon fibers from coal

Carbon fibers carry a great potential for providing several markets with a high strength and light-weight alternative material (2). The automobile industry is highly interested in using carbon fibers to replace heavier materials used throughout various vehicles (3). The reduced weight of the vehicles could significantly improve their fuel efficiency. Further, the inherent inertness and stiffness of carbon fibers lends them to be used for construction purposes, such as bridges and reinforcement materials in concrete. Currently, carbon fibers are mainly obtained from polyacrylnitrile (PAN), a chemical commodity, which has kept the cost of carbon fibers high (4). Therefore, carbon fibers have traditionally been used for applications where price is not prohibitive of introducing superior materials, such as for sports gear and space exploration. However, for the automobile industry the high cost has been a limiting factor. Consequently, fibers from heavy petroleum streams and coal tar pitches have been proposed but are still battling with high costs (5).

The introduction of coal-based carbon fibers has been pursued through various projects funded by CPCPC to reduce costs to a very competitive level. Several technological improvements involving removal of mineral matter by solvent extraction, adjustment of the viscosity, optimization of spinning properties and shortening of the stabilization time needed during carbonization have significantly strengthen the possibility of using coal as feedstock for carbon fibers. Preliminary results indicate that coal-derived carbon fibers can be very cost-effective with competitive fiber properties.

Activated carbon from coal and its combustion by-products

With the ever-expanding market for activated carbons (AC) due to their widespread number of environmental applications, manufacturers of AC are constantly seeking for cost effective and abundant feedstocks. Such feedstocks include coal as well as industrial byproducts (6-8). Traditionally coal is the main precursor for activated carbons produced in U.S. However, carbon from combustion byproducts can also be competitive precursors for AC manufacturers, and simultaneously, reduce waste disposal costs for other industries. One industrial by-product of particular interest is fly ashes of high unburned carbon content from coal-fired combustors. In 2000, about 57 million tons of fly ash was generated by the electric utilities in the U.S. Only about 32% was used mainly for applications in the cement and concrete industries as well as structural fills and waste stabilization applications (9, 10). Unburned carbon has so far hindered the use of most of the remaining fly ash. An increasing role of coal as a source of energy in the 21st century will demand environmental and cost-effective strategies for the use of these carbonaceous waste products from coal combustion. There are already various commercial technologies to separate the unburned carbon from the ash (11, 12). These separation techniques can generate ashes with carbon contents below 6% that are suitable for use in the cement industry, as well as concentrate the unburned carbon that could subsequently be used as feedstock for the production of ACs (13).

Extensive research through CPCPC funded activities has shown that activated carbons with specific surface area up to 1270m^2/g could be produced from the unburned carbon where the porosity of the resultant activated carbons can be related to the properties of the unburned carbon feedstock as well as the activation conditions used. However, not all unburned carbon samples are equally suited for activation since their potential as AC precursors could be inferred from their physical and chemical properties. The developed porosity of the activated carbon also appears to be a function of the oxygen content, porosity and H/C ratio of the parent unburned carbon feedstock. It was further established that extended activation times and high activation temperatures increased the porosity of the produced activated carbon at the expense of the solid yield.

Binders and fillers for carbon products from coal

Many items that we take for granted have some relation to carbon, including aluminum based products where anode carbon is used to reduce the aluminum ore, steel from arc-furnaces using graphite electrodes, and even electric contacts on the key-boards (14). However, the carbon we use is increasingly dependent on the availability of petroleum-derived streams or other foreign sources (15). The decrease in domestic produced oil and the subsequent reliance on imported crude oil may have a serious impact on the future of carbon products and related materials in the US, since most carbon products are typically based on petroleum coke (16). Further, petroleum-derived carbon is also marred by increasing hetero-atom, especially sulfur, and heavy-metal content, and a paradigm shift in the petroleum industry of moving away from producing coke by increasing the use of hydro-cracking and hydro-treatment (17).

The demand for coal tar pitch as a binder for carbon materials is expected to increase with around 3% annually in the coming years (18). A strong driving force for this increase is the Chinese pre-baked anode market that is likely to change from a net exporter in 2002 to a net importer in 2003 as well as a tight coal tar market in Europe. Simultaneously, there is a sharp decrease in coal tar production in US due to the continuous decrease in the production of metallurgic coke caused by environmental and economical reasons. It is also likely that these pressures will decrease the coal tar production in regions such as East Europe and Russia that will further put a pressure on the availability of coal tar binder pitch. Already, synthetic pitches are available that are derived from aromatic monomers. One such example is the AR pitch produced

from naphthalene (19). Naphthalene is reacted at fairly low temperatures (<200°C) at the present of HF and BF_3 to form a oligomeric structure by creating □-bonds between the naphthenic monomers as well as leading to some degree of condensation. However, this pitch prohibitive expensive to be used as a binder for anodes and electrodes. Another solution has been to mix petroleum pitch with coal tar pitch but has received mixed results.

Several projects funded through CPCPC have targeted the reduction in dependence of petroleum coke as filler for carbon materials and import of coal tar pitch for binder purposes by investigating the production of both materials directly from coal. Several advances have been made where solvent extracted material from coal has functioned as a binder as well as a coke precursor (20, 21) and anthracite derived carbon has produced promising candidates for graphite (22, 23).

Future outlook

Emerging markets for carbon products involve energy storage and nano-technology. A great drive towards storage of environmental friendly fuels, such as hydrogen, is taking place in US. Safe storage of hydrogen is of great concern towards the general public. Carbon materials can satisfy this public demand. A vast amount of carbon would be needed to supply every vehicle on the road with adequate storage capacity for hydrogen. Carbon materials derived from coal could easily supply this in an inexpensive and effective manner. Further, the great potential of nano-technology may not be fully achieved if cost-barriers hinder its introduction into the society. Again using coal as a low-cost and abundant starting material may revolutionize the nano-technology era.

Acknowledgement

The Consortium for Premium Carbon Products from Coal (CPCPC) is supported by the U.S. Department of Energy, National Energy Technology Laboratory under the Cooperative Agreement No. DE-FC26-98FT40350.

References

1. Krevelen, D.W. van. *Coal--typology, physics, chemistry, constitution* Elsevier, New York, 1993.
2. Burchell, T. D *Carbon materials for advanced technologies* Pergamon, New York, 1999
3. Chand, S *J. Materials Science* **2000**, *35*, 1303-1313.
4. Marsh, H., Heinz, E.A. and Rodriguez-Reinoso, F. (Eds.) Introduction to Carbon Technologies, Publicaciones Universidad de Alicante, Spain, 1998.
5. Donnet, J.-B. *Carbon fibers* Marcel Dekker, New York, 1998.
6. Patrick, J. W. *Porosity in carbons : characterization and applications* Halsted Press, New York, 1995
7. Haghseresht, F. and Lu, G.Q. *Energy & Fuels* **1998**, *12*, 1100-1107.
8. You, S.Y.; Park, Y.H. and Park, C.R. *Carbon* **2000**, *38*, 1453-1460.
9. Sloss, L.L. *Trends in the use of coal ash* IEA coal research, CCC/22, 1999.
10. Kalyoncu, R.S. *Coal combustion products* US Geological Survery Mineral Yearbook, 2000
11. Ban, H.; Li, T.X.; Hower, J.C.; Schaefer, J.L. and Stencel, J.M. *Fuel* **1997,** 76(8), 801-805
12. Groppo, J.G.; Robl, T.L.; Lewis, W.M.; McCormick, C.J. *Minerals and Metallurgical Processing* **1999**, *16(3),* 34-36.
13. Zhang, Y.; Lu, Z.; Maroto-Valer, M. M.; Andrésen, J. M.; and Schobert, H. H. *Energy & Fuels*, **2002**, submitted.
14. Delhaes, P. *Graphite and Precursors*, Gordon and Breach Sci. Pub., Amsterdam, 2001
15. Farzin, Y.H. *Resource and Energy Economics* **2001**, *23*, 271-291.
16. Marsh, H. *Introduction to Carbon Science* Butterworth & Co Ltd., London, 1989.
17. Speight, J. G.; and Özüm, B. *Petroleum refining processes* Marcel Dekker, New York, 2002.
18. Gipson, J.D., Great Lakes Carbon Corp. 6th Carbon Conf., Sept. 26-28, 2000, Houston, USA, Ch. 9.
19. Korai, Y.; Yoon, S.H.; Oka, H.; Mochida, I.; Nakamura, T.; Kato, I.; and Sakai, Y. *Carbon* **1998**, 36, 369-375.
20. Yang JL; Stansberry PG; Zondlo JW; and Stiller AH, *Fuel Processing Technology* **2002**, *79*, 207-215.
21. Stansberry, P.G.; and Zondlo, J.W. *Prepr. Am. Chem. Soc. Div. Fuel Chem.* **2001**, *46(3)*, 555-556.
22. Andrésen, J.M.; Zhang, Y.; Burgess, C.E.; and Schobert, H.H. *Fuel Processing Technology* **2002**, submitted.
23. Schobert, H.H.; Andresen, J.M.; Pappano, P.J.; Burgess, C.E.; and Zengel, J.J. Pacifichem 2000, Honolulu, Hawaii, USA, December 14-19, 2000, IORG 6, 555.

MECHANICAL PROPERTIES OF CARBON FOAMS DERIVED FROM SOLVENT EXTRACTED CARBON ORE

Elliot B. Kennel
Chong Chen
Peter G. Stansberry
Alfred H. Stiller
John W. Zondlo

West Virginia University
Department of Chemical Engineering
PO Box 6102
Morgantown WV 26506-6102

Introduction

Coal derived feedstocks are economical precursors for fabricating carbon foam.[1,2] Solvent Extracted Carbon Ore (SECO) is produced by first dissolving coal in a dipolar aprotic solvent such as N-methyl pyrrolidone.[3] Insoluble coal solids including the ash are removed by filtration and centrifugation. When the solvent is removed either by evaporation or some other means, the result is an solid organic material. The foam is produced through a controlled coking process. Foaming occurs in a nitrogen or inert gas pressurized autoclave. Because the solvent extracted coal pitch is based on complex, aromatic hydrocarbons, it is expected to form strong bonds upon carbonization and heat treatment, thus making it especially suitable for carbon foam applications.

Experimental

The baseline protocol is to first grind SECO to a mesh size of -50 to -100. The ground SECO is then placed in a non-reactive container, which may be manufactured from ceramic or aluminum. The diameter of the container is limited by the size of the enclave to about 20 cm. The container is placed in a autoclave pressurized to 3.4 MPa with nitrogen. The temperature is ramped at about 2 ^{o}C/min to a peak temperature of 400 ^{o}C to 500 ^{o}C. Outgassing volatiles result in creation of porous foam. The foam is rigidized as the outgassing proceeds. Subsequently, the samples are calcined at 1100 ^{o}C to 1200 ^{o}C at ambient pressure.

Optionally, SECO can be blended with a reinforcement material, which may include, for example, carbon nanofibers, conventional carbon or other fibers.

The samples are recovered and then calcined at 1000 ^{o}C to 1200 ^{o}C in ambient pressure nitrogen or inert gas. This completes the devolatilization as well as cross-linking processes, resulting in improved mechanical properties.

A higher density foam can be created by interrupting the devolatilization process and returning the sample to ambient conditions. The partially foamed SECO is then re-compacted and re-heated. This results in a higher density material with better mechanical properties.

Nanofiber reinforcement was added using carbon nanofibers supplied by Applied Sciences Inc.[4] Nanofibers are carbon filaments with diameters ranging from 50-200 nm and lengths about 100 microns. Sample 8 was wet mixed by incorporating SECO in NMP solvent. All other samples were dry mixed.

Since carbon is exceptionally strong, a network of microspherical carbon structures might also be expected to demonstrate robust mechanical properties.

Results and Discussion

Compression tests were conducted with the use of an Instron device in accordance with ASTM standards, and the results of these tests are shown in Table I. The results indicate that nanofibers act to reinforce carbon foam. However, since the density of the samples also increased as a consequence of nanofiber addition, it is possible that the property improvements were due to increased density rather than contributions from the nanofibers. However, the wet-processed foam (Sample 8) produced superior strength than the dry-processed counterpart (Sample 4). Thus it can be confidently asserted that wet-processed nanofibers, at least, produce enhanced strength in carbon foam over and above any density effects.

Table I. Summary of Compression Results.

Sample Number	Fiber Content	Density, g/cc	Modulus, MPa	Strength, MPa
				MPa
1	0.00	0.491	361	19.8
2	0.697	0.499	481	23.8
3	1.327	0.497	487	23.5
4	2.599	0.509	321	21.8
5	3.862	0.523	501	26.4
6	6.212	0.551	426	25.4
7	7.406	0.577	487	23.2
8	3.829	0.507	448	34.7

Crush Resistance. During compression testing, the sample continues to resist compression after the initial rupture strength S of the sample is reached, though with a lower resistance. The total energy required to crush the sample is taken as the area under the curve, that is,

$$E = \int SALd\varepsilon \quad ,$$

where A is the unit normal area, L is the original thickness of the sample, and ε is the normalized strain. Assuming that the rupture strength is invariant with respect to strain, the rupture energy is simply

$$E = SAL\varepsilon \quad ,$$

the crush energy per unit volume is

$$E_V \equiv \frac{dE}{dV} = S\varepsilon \quad ,$$

and the crush strength per unit mass is

$$E_m \equiv \frac{dE}{\rho dV} = \frac{S\varepsilon}{\rho} \quad .$$

Here ρ is the apparent density.

Assuming a foam with apparent density of 500 kg/m^3, and compressive strength of 3.5 x 10^7 Pa and maximum achievable compressive strain of 0.7, the approximate specific crush energy is 50 kJ/kg. The actual specific crush energy will likely depend upon the energy delivery rate, as well as geometry.

Conclusions

Carbon foams can be created using coal derived feedstocks. Nanofiber reinforcement can be of value in increasing the compressive strength and probably the compressive modulus. Wet mixing of the nanofibers appears to have been more effective than dry mixing. However, the related effect of density increase due to nanofiber addition may also have contributed to the observed improvement in strength.

Acknowledgement. This work was sponsored by the Department of Energy, Contract DE-FC26-01NT41359. Also cited were data from the Office of Naval Research, No.N00014-97-C-0374. Applied Sciences Inc., Cedarville OH, was the source of the nanomaterials for these experiments.

References

(1) Stiller, A. H.; Stansberry; P. G.; and Zondlo; J. W.; US Patent 6,346,226, February 12, 2002.
(2) Stiller, A. H.; Stansberry; P. G.; and Zondlo; J. W.; US Patent 6,183,854, February 6, 2001.
(3) Zondlo, J. W.; Stansberry; P. G.; and Stiller, A. H.; US Patent 5,955,375, September 21, 1999.
(4) Alig R. L.; Kennel, E. B.; Stiller, A. H.; and Zondlo, J. W., Office of Naval Research Contract No.N00014-97-C-0374 Final Report.

COAL AND PETROLEUM BLENDS AS FEEDSTOCK IN THE DELAYED COKING PROCESS TO OBTAIN HIGH VALUE CARBONACEOUS MATERIALS

María M. Escallón, Gareth D. Mitchell, Harold H. Schobert and Mark W. Badger

The Energy Institute, The Pennsylvania State University, University Park, PA 16802

KEYWORDS: Co-coking, delayed coking, mesophase.

Introduction

The delayed coking process has been widely used for the conversion of heavy distillates into lighter ones. Besides obtaining lighter distillates, this process can produce needle coke, a high-value carbonaceous material.

The addition of coal to the decant oil provides more aromatic units to the system; coal components bring both more stability to the distillates [1], and provide to the end coke a better-organized structure. Therefore, the feedstock is converted into a coke via a mechanism involving the formation of mesophase [2].

It is known that the mesophase development plays an important role on the quality of the end-coke. With increasing temperature and, to certain extent, with time at a fixed temperature, the mesophase spheres grow larger [3], leading to the formation of coalesced mosaics with different orientations. This generates more mesophase that leads to anisotropy. The anisotropy is measured by optical microscopy and is the most important parameter to determine the end-use of the coke; the higher anisotropy, the higher is the potential value of the coke.

This work shows the different properties of the coke formed in the delayed coking process at constant temperature and decant oil/coal ratio to determine the best reaction time to obtain a high-value carbonaceous product.

Experimental

The experimental procedure has been previously described [1]. The reactor has three sections, bomb, transfer pipe and catchpot. Approximately 20 g of the mixture decant oil / coal (2:1) was added to the bomb of the reactor. A blank with 20g of pure decant oil was run at six hours to compare the coke obtained with those of co-coking.

The reactor was assembled, purged with N_2 and heated in a sand bath at a constant temperature of 465°C. Reaction times were varied from 2 to 12 hours. At the completion of each timed reaction sequence, the system was cooled at room temperature. The three sections were disconnected. Solids were collected for further evaluation.

The solid product remaining in the bomb was subjected to soxhlet extraction with THF and dried for 1 hour at 100°C in an oven. The characterization of the coke was carried out using a Zeiss Universal Microscope; proximate analyzer, LECO MAC-400; CHN elemental analyzer and total sulfur in a LECO SC-132.

Samples:

Decant oil: Obtained from Seadrift Coke in Texas. This feed is used for making the premium needle coke.

Coal: A number of compatible coals with regard to thermoplastic properties, ash and sulfur values were evaluated in past investigations [1, 4]; it has led to the selection of the Powellton Coal. This coal as was received, was previously cleaned by mechanical processing; this coal is called hereafter as "whole clean Powellton". Another sample of the Powellton coal was obtained from the froth flotation cells at the cleaning plant and subjected to further flotation procedures to reduce the ash yield and sulfur content and maximize the concentration of those components of coal that possess thermoplastic properties. After the cleaning of the "whole Powellton", the sample was stored suspended in water [4]. Sub-samples were removed as slurry and dried at room temperature under a fume hood over a period of four days. Then, it was homogenized and packaged under argon atmosphere. This coal is named hereafter "re-cleaned Powellton froth". Tables 1 and 2 compare some of the properties of the whole clean Powellton coal and the sample taken as slurry, dried and homogenized (re-cleaned Powellton froth).

Table 1. Comparison of Powellton Seam Product with Re-cleaned froth. Proximate and Ultimate Analysis

	Proximate Analysis %			Ultimate Analysis, %			
Analytical Procedure	Fixed carbon	Volatile Matter	Ash	Carbon	Hydrogen	Nitrogen	Total Sulfur
Coal A	65.1	29.9	5.0	87.6	5.8	1.6	0.9
Coal B	68.7	29.4	1.9	86.3	5.2	1.5	0.9

Table 2. Comparison of Powellton Seam Product with Re-cleaned froth. Plasticity and Maceral Content.

	Gieseler Plastometer		Organic Petrography, vol.%		
Analytical Procedure	T. at maximum fluidity (°C)	ddpm	Vitrinite	Liptinite	Inertinite
Coal A	448	30,000	68.0	8.6	23.4
Coal B	448	23,619	88.1	2.0	9.9

A: Whole clean Powellton
B: Re-cleaned Powellton Froth

It is important to notice from the tables that the whole clean Powellton showed a higher fluidity compared to the Re-cleaned Powellton, even though both samples are derived from the same coal and cleaning facility. The lower fluidity can be attributed to the finer particle size of the Re-cleaned Powellton Froth as well as to oxidation during storage.

Results and Discussion

Volatile Matter. This is a good parameter to compare the product coke quality, especially for metallurgical coke. As reaction time increased, volatile matter decreased (figure 1). The volatile matter of the coke derived from the decant oil (100%) at a reaction time of 6 hours has the higher volatile matter of the entire samples tested (56% volatile matter).

THF Solubles. The soxhlet-extracted cokes have been analyzed by microscopy and ultimate/proximate. It is noteworthy that the amount of THF solubles in the coke is reduced as reaction time is increased. This indicates that at higher reaction times, coal is giving more volatile compounds to the liquids, making of the solid at

higher reaction times a better coke, visibly darker and more difficult to be broken.

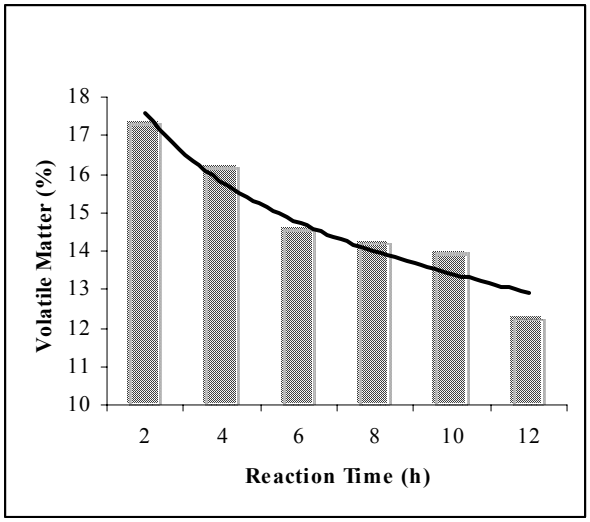

Figure 1. Volatile Matter vs. Reaction Time. Decant oil/coal 2:1 ratio.

Comparison Whole clean Powellton with Re-cleaned Powellton Froth. Both samples expose the same behavior for volatile matter and liquid and solid yields but microscopically, whole clean powellton shows a better interaction with the decant oil.

Acknowledgement. The authors are pleased to acknowledge the financial support for this work provided by the Air Force Office of Scientific Research. We thank Seadrift Coke for the sample of decant oil used in this work. We also thank Dr. Barbara J. Arnold, PrepTech, Inc., for technical advice and the froth flotation separation.

References

(1) Fickinger A. M.S. Thesis, the Pennsylvania State University, **2000**.
(2) Martinez-Escandell M., et. al., *Carbon*, **1999**, 37, 1567-1582
(3) Chemistry and Physics of Carbon; P L. Walker Jr. Ed. Marcel Dekker, Inc, N.Y., 1968, vol. 4. "The formation of some graphitizing carbons" by Brooks JD and Taylor GH. **1968**. 243-286.
(4) Badger, M., Mitchell G., Final Report **2001** – Co-coking of Coal/Decant Oil Blends. The Pennsylvania State University – The Energy Institute.

CARBON AS CATALYST FOR ORGANIC ELECTRON-TRANSFER REACTIONS

Francelys A.Medina, John W. Larsen and Harold H. Schobert

The Energy Institute, The Pennsylvania State University, University Park PA 16802

Introduction

Carbons catalyze a variety of reactions.[1,2] Because of their low cost and wide variety of reasonably well-defined physicochemical properties and morphologies, carbons are desirable catalytic materials. However, little systematic attention has been given to their use and behavior as catalysts and we have initiated a research program to understand the fundamentals of carbons as catalysts. We address here two carbon catalyzed reactions (Eq. 1 and 2 below) for which there exists some mechanistic information: the reduction of nitrobenzene to aniline by hydrazine[3] and the decomposition of hydrazine.[4] These reactions are thermodynamically highly favorable, but do not readily proceed at a measurable rate in homogeneous solution due to kinetic barriers.[5] The nitrobenzene reduction follows the overall equation,

$$2PhNO_2 + 3N_2H_4 \xrightarrow{C} PhNH_2 + 4H_2O + 3N_2. \qquad (1)$$

The decomposition of hydrazine also yields gas products,

$$N_2H_4 \xrightarrow{C} 4/3\ NH_3 + 1/3\ N_2 \qquad (2)$$

Thus, the kinetics can easily be followed by measuring gas production as a function of time.

Experimental

Carbon Samples. The carbon samples that were examined in this study include carbon blacks (Cabot Corp.), activated carbons (MeadWestvaco Corp.), non-activated charcoals and graphite (Fisher Scientific). They were used as received. The BET surface area was determined by N_2 physisorption at 77 K using a Quantachrome Autosorb 1 analyzer. Elemental analysis of the carbon samples was carried out with a LECO CHN-600 elemental analyzer, a LECO SC-132 sulfur determinator and a LECO MAC-400 proximate analyzer.

Kinetic measurements. All compounds were obtained from Fisher Scientific and were used without purification. Reactions were carried out by adding hydrazine to a refluxing solution of nitrobenzene and carbon in *iso*propanol under a N_2 atmosphere. In the decomposition of hydrazine reaction, nitrobenzene was not added to the reaction mixture. The reactions were followed by measuring gas volumes as a function of time using a gas burette.

Results and Discussion

Typical results for nitrobenzene reduction using different carbons as catalysts are shown in **Figure 1**, plotted as gas volume evolution vs. time. The production of gases upon addition of carbons to otherwise stable solutions of the reactants demonstrates that the carbons tested catalyze the nitrobenzene reduction by hydrazine, although with different activities. For each carbon, the gas evolution plots show simple time dependence. The kinetics are complex as evidenced by deviations from first-order reactions for higher activity carbons and from second-order reactions for lower activity carbons. This is not surprising for a heterogeneous bimolecular reaction

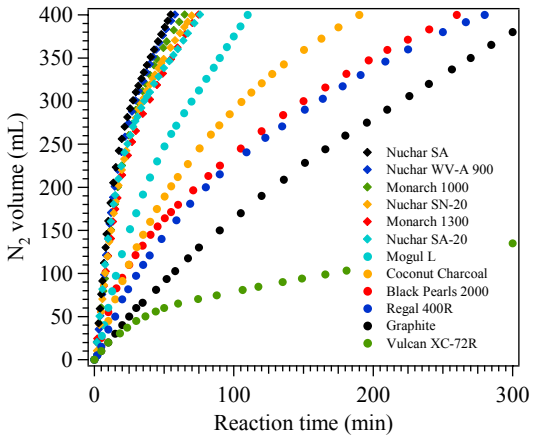

Figure 1. Gas evolution from carbon-catalyzed nitrobenzene reduction in the presence of hydrazine. Legend shows the approximate plot order from top to bottom.

The observed activity (activated carbons > carbon blacks > natural charcoals > graphite), determined by the initial rate, generally parallels the BET surface area of the carbon catalysts as shown in **Figure 2**. In general, the initial rate increases with the surface area of the carbon catalyst. However, there is not a straightforward relationship between the BET surface areas of the carbons in **Figure 2** and the rates of nitrobenzene reduction. This indicates that other factors are important for catalysis on these carbons. The best candidates for these factors are the amount and the type of surface groups. It is well known that different carbons have different surface functionality depending on the nature and the mode of formation of the carbon samples.

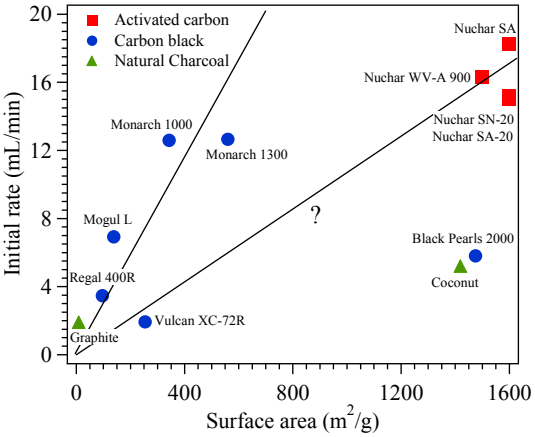

Figure 2. Influence of surface area on the rate of nitrobenzene reduction by hydrazine on various carbons.

The results in **Figure 3** demonstrate that the rate of nitrobenzene reduction increases with increasing total oxygen content of the catalyzing carbon. Because the total oxygen content is plotted, no information is available about the relative importance of different oxygen functional groups. The fact that the reaction rate differs considerably for activated carbons with similar oxygen contents indicates that not all of the oxygen functional groups are equally important to this reaction. Infrared analysis can be used to provide additional information on the types of oxygen functional groups that are present on the carbon samples.

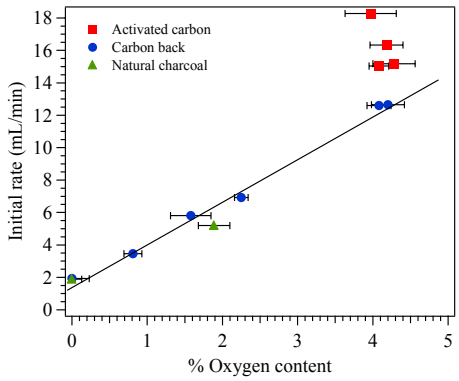

Figure 3. Influence of oxygen content of the rate of nitrobenzene reduction by hydrazine on various carbons. Oxygen concentration was obtained from elemental analysis. Solid line indicates the trend of the data.

As shown in **Figure 4**, the reaction rate initially increases with nitrobenzene concentration and goes through a maximum before falling off at the higher concentrations, in agreement with a Langmuir-Hinshelwood surface-controlled reaction model.[6] According to this model, the rate of nitrobenzene reduction is limited by the degree of adsorption of both nitrobenzene and hydrazine on the carbon catalysts. This observation supports the idea that carbon serves as an adsorbent.[3]

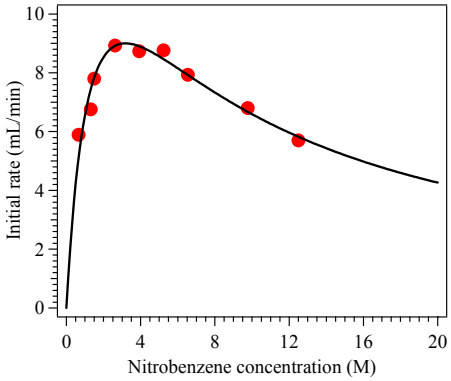

Figure 4. Variation of nitrobenzene reduction rate with nitrobenzene concentration. Black Pearls 2000 was used as catalyst. Solid line indicates the trend of the data

Figure 5 shows the gas volume evolved vs. time for solutions of hydrazine in refluxing *iso*propanol with different carbons added. As in the case of the nitrobenzene reduction, we found that all of the carbons catalyze the reaction to different extents. The reaction rate for the nitrobenzene reduction is directly proportional to the rate of the hydrazine decomposition and faster by a factor of ten or more. When both reactions proceed simultaneously, the contribution to the gases evolved from hydrazine decomposition does not affect significantly the nitrobenzene reduction kinetics. Under the reaction conditions used in this experiment, the decomposition of hydrazine on carbons was found to be a third-order reaction, as shown in **Figure 6**. The mechanism is not known yet, however, the existence of third order kinetics for hydrazine decomposition on carbons is similar to electrochemical results on glassy carbon electrodes showing that three molecules of hydrazine are involved in hydrazine decomposition.[7]

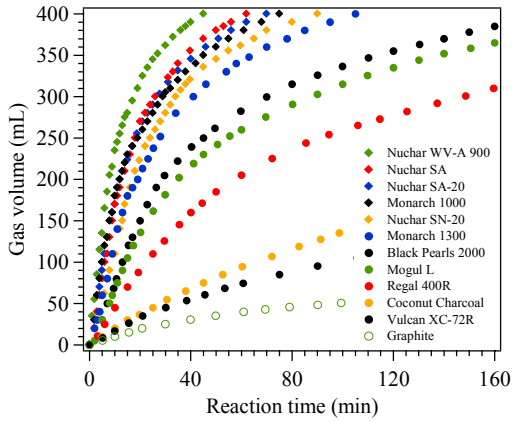

Figure 5. Gas evolution from carbon-catalyzed decomposition of hydrazine. Legend shows the approximate plot order from top to bottom.

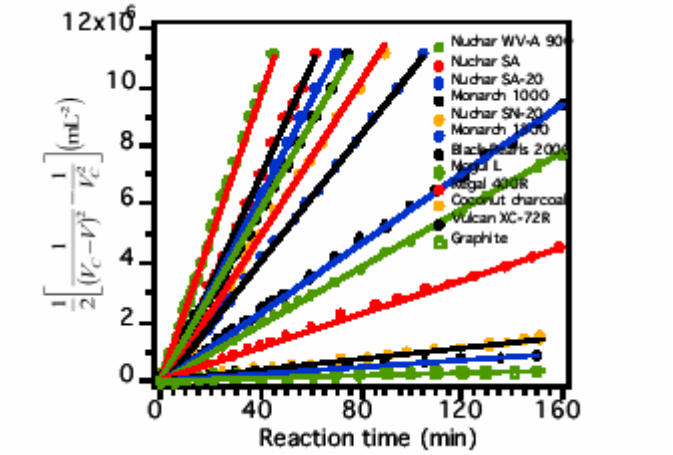

Figure 6. Kinetics of the carbon catalyzed decomposition of hydrazine plotted as a third order reaction (V, gas volume at time t; V_C, calculated final gas volume using the stoichiometric of Eq. 2).

Conclusions

The results obtained in this study demonstrate a correlation between the reaction rate and the physicochemical properties of the carbon catalyst. In particular, the oxygen groups that are present on the carbons surface are believed to participate in the nitrobenzene reduction by hydrazine, and their presence may enhance the reaction rate.

The physical chemistry of carbon materials may indeed make a decisive contribution to their catalytic properties by the determination of the quantitative and qualitative features of active sites. Thus, by changing these parameters in a wide range it is possible to vary the catalytic properties of carbon materials.

References

(1) Spiro, M. *Catal. Today* **1990**, *7*, 167-178.
(2) Radovic, L. R.; Rodriguez-Reinoso, F. In *Chemistry and Physics of Carbon*; Thrower, P. A., Ed., 1997; Vol. 25, pp 243-358.
(3) Larsen, J. W.; Freund, M.; Kim, K. Y.; Sidovar, M.; Stuart, J. L. *Carbon* **2000**, *38*, 655-661.
(4) Larsen, J. W.; Jandzinski, J.; Sidovar, M.; Stuart, J. L. *Carbon* **2001**, *39*, 473-476.
(5) Furst, A.; Berlo, R. C.; Hooton, S. *Chem. Rev.* **1965**, *65*, 51.
(6) Laidler, K. J. *Chemical kinetics*; 3rd ed.; Harper & Row: New York, 1987.
(7) Cao, X.; Wang, B.; Su, Q. *J. Electroanal. Chem.* **1993**, *361*, 211-214.

THE MUTIPLE SITE MODEL FOR FLUE GAS–MERCURY INTERACTIONS ON ACTIVATED CARBONS: THE BASIC SITE

Edwin S. Olson, Jason D. Laumb, Steven A. Benson, Grant E. Dunham, Ramesh K. Sharma, Stanley J. Miller, and John H. Pavlish

Energy & Environmental Research Center
University of North Dakota
Box 9018
Grand Forks, ND 58202

Introduction

The control of mercury emissions in flue gas from coal-burning utilities continues to be an important issue. Powdered activated carbons (ACs) prepared from coal precursors are effective sorbents under these flue gas conditions, but further advances in understanding the chemisorption mechanisms are needed to better design carbons with faster kinetics and greater capacities. The commercial powdered carbon Norit FGD sorbent has been thoroughly investigated at the Energy & Environmental Research Center (EERC) as a sorbent for elemental mercury (Hg^0) in flue gas streams (1, 2). Extensive factorial evaluations of powdered sorbents were conducted in a bench-scale system consisting of a thin fixed-bed reactor in gas streams containing 15 μg/m^3 of Hg^0 in various simulated flue gas compositions consisting of acidic SO_2, NO_2, and HCl gases plus a base mixture of N_2, O_2, NO, CO_2, and H_2O (1). In an atmosphere containing HCl or NO_2, the Norit FGD, which is a Texas lignite-derived AC, was effective for capture of Hg^0 from the gas phase at temperatures of 100° to 150°C. Without either HCl or NO_2 in the gas stream, the carbon sorbents are ineffective, and immediate breakthrough occurred.

In tests conducted with the FGD sorbent in the simulated flue gas containing NO_2 but not SO_2, very little breakthrough was observed over an extended time period, indicating that the bound mercury form is quite stable. The capture is attributed to oxidation of the Hg^0 and concomitant reduction of NO_2 with formation of a low-volatile oxidized mercury species that remains bonded to the sorbent (3). Reactions of Hg^0 with NO and NO_2 in a glass container were previously reported to form mercuric oxide and mercuric nitrate–nitrite mixtures (4). When SO_2 was added to the gas mixture containing the NO_2, the mercury sorption rate was initially high (98% of inlet Hg^0 was sorbed); however, breakthrough occurred at times inversely proportional to the concentration of SO_2; that is, the higher the concentration of SO_2 is, the shorter the breakthrough time. With typical flue gas SO_2 concentrations (1500 ppm), the breakthrough occurs after 1 hour at the 107°C conditions. The breakthrough curve was relatively steep, increasing to 100% or greater emission after about 2 hours. Thus, not only is mercury no longer sorbed, but mercury sorbed earlier in the experiment is released. Similar interactions were observed for ACs produced from Fort Union lignites under certain similar conditions (5). These breakthrough capacity results are consistent with the hypothesis that SO_2 poisons the binding site for Hg(II) on the sorbent surface.

The Dual-Site Model for Mercury–Flue Gas Interactions with FGD Sorbent

An important fact leading to the development of a model for the interactions occurring on the carbon surface is that the mercury that is emitted from the sorbent after breakthrough is entirely an oxidized mercury species. This was noted when the converter on the continuous emission monitor was taken off after breakthrough and the Hg signal dropped from 100+% emission to close to 0%. Furthermore, in reactions conducted with NO_2 and SO_2 and no HCl, this emitted volatile oxidized mercury product was actually trapped and identified as mercuric nitrate (6, 7).

We, therefore, postulated that the carbon sorbents have two or more independent reaction sites comprising at least an oxidation site and a binding site for the oxidized Hg (8). By definition, the oxidation site is an electron-accepting Lewis acid site, and the Hg (II) binding site is an electron-donating basic site. Poisoning of the binding site by acid components from the flue gas at breakthrough does not affect the functioning of the oxidation site. Thus the mechanistic multiple site model shown in Figure 1 is proposed (5). It should be noted that there could be additional separate sites for NO_2 reduction, SO_2 oxidation, and oxygen reduction (the latter two are omitted from the diagram for simplicity).

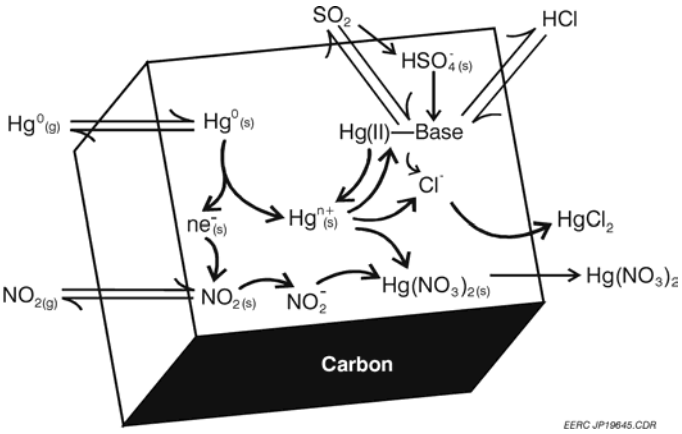

Figure 1. Mechanism for mercury capture on FGD sorbent.

The location, structure, and mechanistic functioning of the oxidation and binding sites are of great importance in understanding the mercury–flue gas interactions. Of interest is the question of whether the extensive mineral matter (35%) of the FGD sorbent contributed to the Hg binding. Recent EERC data show that sequential removal of the inorganic matter from the FGD sorbent did not significantly affect the breakthrough behavior (8); thus the basic groups, such as calcium oxide present in the FGD sorbent, played no role in the mercury–flue gas interactions that determine the breakthrough capacity. Thus the binding site was postulated to be a Lewis basic site residing on the carbon surface. The nature of this binding site is the subject of this paper.

Summary of X-Ray Photoelectron Spectroscopy Analysis of Flue Gas-Exposed Sorbents

Further insights into the mechanisms of the mercury–flue gas–sorbent interactions were derived from the x-ray photoelectron spectroscopy (XPS) data obtained from two AC sorbents, Norit FGD and the EERC lignite-derived AC, exposed to various simulated flue gas compositions containing Hg^0 with various levels of SO_2, NO_2, HCl, and H_2O for time periods before and after breakthrough of mercury (9). Because of the interference caused by silicon, XPS data could not be obtained for the mercury species present in the exposed sorbents. However, information on the forms of sulfur and chlorine was especially important in understanding the interactions. The conclusions from the detailed, high-resolution XPS scan spectroscopic study are summarized here.

The XPS analysis indicated that sulfur(VI) (sulfate or bisulfate) is the major sulfur species on all the sorbent samples exposed to flue gas compositions. The longer the exposure to SO_2, the more sulfate is found in the sample. When NO_2 was omitted from the flue gas, less sulfate was accumulated. A decrease in sulfate was also observed

when H_2O was omitted from the gas composition. The presence or absence of HCl had no effect on the sulfate formed. Based on these analyses, several adsorption as well as chemisorption events must occur during the exposure of carbon sorbents to flue gas components. The adsorbed SO_2 is clearly oxidized on the sorbent surface, resulting in bound bisulfate. The continued accumulation observed for sulfate or bisulfate should occur at basic sites, including basic sites on carbon that are responsible for binding the Lewis acid Hg(II). This is consistent with the large sensitivity of Hg breakthrough observed for SO_2 concentrations. Physical pore blockage by sulfate cannot explain the poisoning, because that would also block the oxidation sites. The oxidation of SO_2 is influenced strongly by the availability of NO_2, a good oxidizing agent. Although O_2 may also serve as the electron sink, the reaction in the absence of NO_2 gives much less sulfate. These data also indicate that the SO_2 oxidation reaction involves water.

The XPS data showed that chlorine is present as both chloride ion and covalent (organic) chlorine. If mercuric chloride were present on the surface, the very small amount could not be seen owing to the interference of these forms. More chlorine was present on the exposed sorbent when no SO_2 was used in the gas composition. Importantly, the chlorine forms disappear from the carbon surface when breakthrough occurs. Thus the HCl in the flue gas can donate a hydrogen ion to a basic site, as well as add both hydrogen and chlorine to a basic site to form the organochlorine product. This addition is well-known in olefin chemistry where alkyl halides are formed. The accumulation of chlorine in the absence of SO_2 as well as the disappearance of chlorine after continued exposure in SO_2 is explained by competition of HCl with bisulfate. As more bisulfate is generated from SO_2 at the carbon surface, it displaces the HCl, owing to the high volatility of HCl.

Model for the Lewis Basic Binding Site for Hg(II)

A refinement of the Lewis acid basic binding site model is now proposed that offers more detail on the nature of the carbon site and its interaction with flue gases and Hg. This model uses the concept of zig-zag carbene structures recently proposed for electronic states at the edges of the carbon graphene layers (10). An alternative, plausible mechanism can be proposed for the armchair sites, but is not presented here.

In the carbene model, the zig-zag carbon atom positioned between aromatic rings is assumed to be the Lewis base site. Aliphatic and haloaliphatic carbenes are always highly electrophilic as exhibited by rapid addition reactions to alkenes and sigma bonds. In contrast, heteroatom and aromatic substituted carbenes are in fact nucleophilic, exhibiting no reactivity to alkenes or reactivity to alkenes with electron-withdrawing groups, respectively.

The interactions that appear to be adequate for explaining the behavior of the FGD sorbent are summarized in more detail in the scheme shown in Figure 2. Thus, in the proposed model for the basic site, the zig-zag Lewis basic carbene reacts with the oxidized Hg species (postulated as a mobile "spill-over" species like mobile hydrogen). But the basic carbene also reacts with HCl, H_2SO_4, and SO_2 to form the bound chlorine, sulfate, and sulfinate as demanded in the XPS results. The reaction is thus a reversible addition of hydrogen ion from the acid to the carbene to form carbenium ion intermediates, which subsequently bond to the anion. Flue gas interactions occurring at the Lewis acid oxidation site on the carbon are currently under investigation.

Acknowledgments

Support is gratefully acknowledged from the EERC Center for Air Toxic Metals[K] Industrial Affiliates Program.

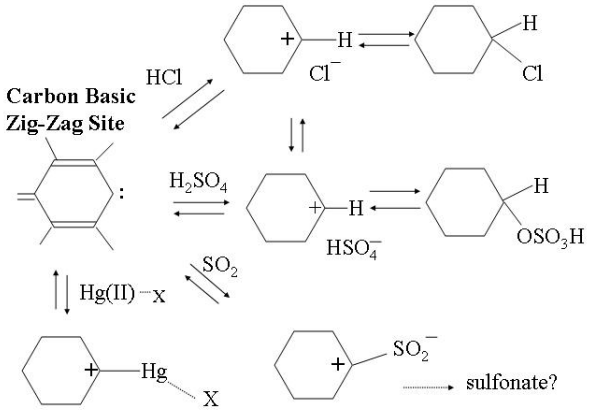

Figure 2. Basic site model.

References

(1) Miller, S.J.; Dunham, G.E.; Olson, E.S.; Brown, T.D. Flue Gas Effects on a Carbon-Based Mercury Sorbent. In *Air Quality: Mercury, Trace Elements, and Particulate Matter*, Special Issue of *Fuel Process. Technol.* **2000**, *65–66*, 343–363.

(2) Miller, S.J.; Dunham, G.E.; Olson, E.S.; Miller, S.J. Impact of Flue Gas Constituents on Carbon Sorbents. In *Proceedings of the Air Quality II: Mercury, Trace Elements, and Particulate Matter Conference*; McLean, VA, Sept 19–21, 2000; Paper A4-3.

(3) Olson, E.S.; Miller, S.J.; Sharma, R.K.; Dunham, G.E.; Benson, S.A. *J. Hazard. Mater.* **2000**, *74*, 61–79.

(4) Freeman, E.S.; Gordon, S. *J. Amer. Chem. Soc*. **1956**, *78*, 1813.

(5) Olson, E.S.; Sharma, R.K.; Eylands, K.E.; Stepan, D.J. Fuel Chem. Div. Prepr. 2002, 47(2), 472.

(6) Olson, E.S.; Sharma, R.K.; Miller, S.J. Dunham, G.E. Mercury in the Environment. In *Proceedings of a Specialty Conference*; VIP-91, Air & Waste Manag. Assoc., Minneapolis, MN, Sept 15, 1999; p 121.

(7) Olson, E.S.; Thompson, J.S. Cryogenic and Solvent Trapping of Oxidized Mercury Species in Flue Gas. In *Proceedings of the EPA–DOE–EPRI Combined Power Plant Air Pollutant Control Symposium: "The Mega" Symposium*; Chicago, IL, Aug 21–23, 2001; Session 16, No. 212.

(8) Olson, E.S.; Dunham, G.E.; Sharma, R.K.; Miller, S.J. *Prepr. Pap.—Am. Chem. Soc., Div. Fuel Chem.* **2000**, *45* (4), 886.

(9) Laumb, J.D.; Benson, S.A.; Olson, E.S.; Dunham, G.E. Characterization of Coal-Derived Mercury Sorbents. Presented at the 26th International Clearwater, FL, March 5–8, 2001.

(10) Radovic, L.R.; Bockrath, B. *Fuel Chem. Div. Prepr.* **2002**, *47* (2), 428.

ACTIVATED CARBONS PRODUCED FROM UNBURNED CARBON IN FLY ASH AND THEIR APPLICATION FOR MERCURY CAPTURE

Yinzhi Zhang[1], Evan J. Granite[2], M. Mercedes Maroto-Valer[1], and Zhong Tang[1]

[1]The Energy Institute and Department of Energy and Geo-Environmental Engineering, The Pennsylvania State Univrstiy, 405 Academic Acativities, University Park, PA 16802
[2]National Energy Technology Laboratory, United States Department of Energy, P.O. Box 10940, Pittsburgh, PA 15236-0940

Introduction

Following the current demand to develop technologies to utilize high carbon content fly ash from coal-fired utility combustors or gasifiers, a one-step activation protocol has been developed by the authors to produce activated carbons from unburned carbon in fly ash[1-3]. Compared to the conventional two-step process that includes a devolatilization of the raw materials, followed by an activation step, unburned carbon only requires a one-step activation process, since it has already gone through a devolatilization process while in the combustor or gasifier. The produced activated carbons with a fine particle size are not only rich in micropores, but they also present a high content of mesopores, which leads to good mass transfer properties during the adsorption process.

Mercury has been identified as a hazardous air pollutant of greatest potential public health concern by the Environmental Protection Agency (EPA), with coal-fired utility boilers being the largest source of anthropogenic mercury emissions[4,5]. Based upon the EPA report, in 1997 it was estimated that 48 tons of mercury were emitted into atmosphere from coal-fired utilities, including 26 tons of elemental mercury and 20.5 tons of oxidized mercury, and where the state of Pennsylvania emitted around 5 tons[6]. The injection of carbon adsorbent upstream of the electrostatic precipitator (ESP) or baghouse particulate collection devices is a promising technology to control mercury emissions from coal-fired combustion systems[7]. A large excess of carbon adsorbent is normally required for injection upstream of the ESP or baghouse in order to obtain a high level of mercury capture. This is because the concentration of mercury in the flue gas is extremely low, (on the order of 1 ppb by volume[8]), as well as the complexity of the flue gas composition and the poor selectivity of the carbon sorbent towards mercury. The typical carbon-to-mercury mass ratios used in recent pilot-scale studies of mercury capture in power plant systems were between 1000:1 to 100,000:1[7,8]. Therefore, the cost of the carbon sorbent plays an important role in the feasibility of the proposed technologies. Based on the low cost of fly ash carbon, its inherent porosity together with its fine particle size, the unburned carbon has been tested as a potential mercury sorbent candidate[8,9]. However, its mercury capacity is lower than that of commercial carbons, probably due to its high ash content and low surface area. Accordingly, the present paper focuses on the activation of the unburned carbon after conventional demineralization process in order to increase the porosity of the unburned carbon. In addition, the prepared activated unburned carbon samples were tested for mercury adsorption using a fixed-bed with a simulated flue gas at 280°F.

Experimental

Six unburned carbon samples, named DA, FA1, PO, SH, WE and CFA were collected from different combustors, including pulverized coal units and cyclone units.

Beneficiation of fly ash carbons. The unburned carbon content of fly ash samples SH were enriched by using conventional froth flotation methods and reagents. A 2.5-liter WEMCO laboratory froth flotation cell and coal froth flotation reagents were used, including several scavenger stages to remove additional carbon from the ash product and various cleaning stages to reduce the ash content in the carbon product. A sink/float test was also conducted with fly ash sample FA1 in order to determine the feasibility of using sink/flotation techniques to separate the unburned carbon from the fly ash. In addition, an acid digestion step was also conducted by following conventional $HCl/HNO_3/HF$ treatment to further reduce the ash content in the carbon concentrate.

Characterization of the samples. The loss–on-ignition (LOI) contents of the fly ash samples were determined according to the ASTM C311 procedure. The porosity of the samples was characterized by conducting N_2 adsorption isotherms at 77K using a Quantachrome adsorption apparatus, Autosorb-1 Model ASIT. The pore volume was calculated from the volume measured in the nitrogen adsorption isotherm at a relative pressure of 0.95 ($V_{0.95}$). The total specific surface area, S_t, was calculated using the multi-point BET equation in the relative pressure range 0.05-0.35, as described previously[10,11].

Production of activated carbon by one-step activation. The activation of the samples was carried out in an activation furnace consisting of a stainless steel tube reactor inside a vertical tube furnace, as previously described[2]. The sample was heated under nitrogen flow to the desired temperature, and then steam was introduced in the reactor, while the reactor was kept under isothermal conditions for 1-3 hours.

Mercury adsorption tests. A detailed description of the assembly and instruments used for testing the mercury capacity of unburned carbon samples and their activated counterpart can be found elsewhere[8]. The system features an elemental mercury permeation tube, a flue gas blending system, an elemental mercury detector (atomic fluorescence spectrophotometer), and digestion of used sorbents by cold vapor atomic absorption spectrophotometry.

Results and Discussion

Cleanability of fly ash carbons. The feedstock used for the froth flotation test was sample SH, which was collected from a cold-side hopper in a pulverized coal combustion unit, and had an initial LOI content of around 44%. As expected, the scavenger tailings had the lowest level of carbon at 23% and a yield of 48%; while the products from the final recleaner stage contained about 75-76% carbon and have a yield of 21%. Therefore, froth flotation can be used for the separation of fly ash into a carbon and an ash stream. The feedstock used for the sink/float test was sample FA1 with an initial LOI of around 59% and the separation results are listed in Table 1.

Table 1. Sink/float separation results for sample FA1.

Sample	LOI, %	Yield, %
1.6 float	84.9	1.8
1.6 sink	64.7	98.2
1.7 float	83.7	1.6
1.7 sink	64.8	98.4
1.8 float	86.5	6.5
1.8 sink	63.3	93.5
1.9 float	86.6	31.3
1.9 sink	53.4	68.7
2.2 float	72.7	86.0
2.2 sink	20.3	14.0
2.5 float	67.2	96.1
2.5 sink	31.2	3.7

The data in Table 1 shows that using a conventional density liquid medium, unburned carbon can be separated from ash at different purity levels. For example, using the medium with density of 2.2 g/ml, an ash stream with the lowest carbon content (20.3%) can be obtained. On the other hand, a carbon stream with a low ash content (around 13-14%) can be obtained by using a wide range of media (density 1.6-1.9 g/ml), where using the 1.9g/ml medium the carbon stream has highest LOI (86.6%) together with the highest yield (31.3%). Chemical digestion was also conducted on fly ash sample FA1 using $HCl/HNO_3/HF$ treatment, and the resultant fly ash carbon stream has an ash content of only ~1%.

Porosity of the fly ash samples. The LOI values and the total surface area and pore volume of the six fly ash carbon calculated from 77K nitrogen isotherm are presented in Table 2. For the purpose of comparison, all the data have been converted into dry ash-free basis. The LOI values range from 46-87wt%. The LOI values reported here are higher than those reported in previous studies that are typically around 15wt%. However, this work focuses on the characterization of high carbon fly ashes for their subsequent use as feedstock for activated carbons, and therefore, samples with high LOI contents were intentionally selected.

Table 2. LOI and porosity of the fly ash samples.

Sample	LOI %	S_t m^2/g	$V_{0.95}$ ml/g	D_{av}, nm
DA	50.0	35	0.032	3.69
WE	32.0	48	0.040	3.35
PO	50.8	51	0.046	3.60
SH	45.8	39	0.036	3.76
FA1	58.9	125	0.077	2.45
CFA	86.6	18	0.019	4.31

The specific surface areas for unburned carbon samples collected from different units range from 18 to 125 m^2/g. The sample FA1, one of the samples from pulverized coal unit, has the highest surface area and pore volume of 125 m^2/g and 0.077 ml/g, respectively. This suggests that the sample FA1 has already generated certain porosity while in the combustor prior to the activation process. On the other hand, the sample from cyclone combustor has the smallest surface area and pore volume of 18 m^2/g and 0.019 ml/g, respectively. This could be due to the higher temperature experienced in the cyclone[13] for CFA compared to the other samples from PC units. Microporosity in carbons is well known to be dependent on the heat treatment temperature and the heating rate experienced by the coal particles in the different furnace[14, 15]. In addition to temperature and heating rate, another factor that could influence the porosity development in the unburned carbons is the mineral composition, which may have a catalytic effect on carbon gasification reactions[16].

One-step activation. Table 3 shows the surface area and pore volume for the activated carbon from the six samples investigated here. As described for the data presented in Table 2, the data have been corrected into dry ash-free basis. The samples were steam activated at 850°C for different periods of time until the burn-off was around 70%, except for CFA, whose burn-off is only around 37% even after 3 hours activation, probably due to its low reactivity.

Compared to the porosity data in Table 2 for the parent unburned carbon, for all the samples the one-step steam activation process has successfully increased the surface area and pore volume. For example, the unburned carbon sample WE has a surface area of only 48 m^2/g, while its activated counterpart has a surface area of approximately 800m^2/g. The activated carbon from sample FA1 has the highest surface area of ~1200 m^2/g, which is comparable to typical commercial activated carbons like F-400 with a surface area of around 1200 m^2/g[11]. Mercury adsorption tests will be conducted and their adsorption capacities will be compared to those obtained for conventional activated carbons.

Table 3. Surface area and pore volume of activated unburned carbons.

Sample	S_t m^2/g	$V_{0.95}$ ml/g	D_{av}, nm
AC-DA	540	0.556	4.05
AC-WE	803	0.647	3.22
AC-PO	499	0.514	4.12
AC-SH	242	0.221	3.64
AC-FA1	1273	0.815	2.56
AC-CFA	157	0.153	3.88

Conclusions

The unburned carbon collected from coal-fired combustors can be separated from the ash by conventional froth/flotation and sink/float methods. By applying acid digestion, a high purity unburned carbon with an ash content less than 1% can be obtained. The one-step activation process can dramatically increase the surface area and pore volume of the carbon. The resulting activated carbons possess surface areas greater than 1200 m^2/g, which is comparable to many commercially available activated carbons.

Acknowledgements

The authors wish to thank the Consortium for Premium Carbon Products from Coal (CPCPC) at The Pennsylvania State University for financial support, and to Dr. Mark Klima (Penn State University) and Dr. Barbara Arnold (Prep Tech) for their help with the cleanability studies.

References

(1) Maroto-Valer, M.M.; Taulbee, D.N. and Hower, J.C. *Energy & Fuel*, **1999**, *13,* 947.
(2) Maroto-Valer, M.M.; Taulbee, D.N. and Schobert, H.H. Prepr. Pap. - *Am. Chem. Soc., Div. Fuel Chem.*, **1999**, *44* (1), 101.
(3) Maroto-Valer, M.M.; Taulbee, D.N. and Schobert, H.H. *Proceedings of the 24th Biennial Conf. On Carbon,* **1999**, *1,* 588
(4) DOE fossil energy – mercury control technologies – fact sheet: http://fossil.energy.gov/coal_poer/existingplants/mercurycontrol_fs.shtml, Sept. 6, **2002**
(5) U.S. EPA mercury web site: general information, http:// www.epa.gov/mercury /information.htm#fact_sheets, May 17, 2002
(6) EPA report: Emission of mercury by state, **1999**.
(7) Activated carbon injection for mercury control in coal-fired boilers, Newsletter of center for air toxic metals, Energy and environmental research center in University of North Dakota, 6(1), May **2000**.
(8) Granite, E.J.; Pennline, H.W. and Hargis, R. A. *Ind. Eng. Chem. Res.* **2000**, *39*, 1020-1029
(9) Hwang, J.; Li, Z. U.S. Patent 6027551, **2000**
(10) Zhang, Y.; Wang, M.; He, F. and Zhang, B. *J. Mater. Sci.* ***1997,*** *32*,6009
(11) Zhang, Y.; Maroto-Valer, M.M.; Tang, Z.; Lu, Z.; Andrésen, J.M. and Schobert, H.H. *Proceedings of 19th annual international Pittsburgh coal conference,* paper 126.pdf, **2002**
(12) Zhang, Y.; Lu, Z.; Maroto-Valer, M.M.; Andrésen, J.M. and Schobert, H.H., Energy & Fuel, in press.
(13) Boram, G.L.and Ragland, K.W. *Combustion Engineering,* WCB McGraw-Hill, **1998**
(14) Marsh, H. and Wynne-Jones, W.F.K. *Carbon,***1964**, *1*, 269
(15) Marcilla, A.; Asensio, M. and Martin-Gullon, I. *Carbon* **1996**, *34,* 449
(16) McEnaney, B. Active sites in relation to gasification of coal chars, *Fundamental issue in control of carbon gasification reactivity,* Edited by Lahaye, J. and Enrburger, P., Kluwer Academic Publishers, **1991**, 175

EFFECTS OF ACTIVATION CONDITIONS ON THE ACTIVITY OF CARBONS FROM FORT UNION LIGNITES

Ramesh K. Sharma and Edwin S. Olson

Energy & Environmental Research Center
University of North Dakota
PO Box 9018
Grand Forks, ND 58202

Introduction

Activated carbon has been prepared from coals of various ranks and types, but the highly reactive Fort Union lignites have not been utilized commercially for preparing adsorbent carbons or other useful carbons. We recently reported that the high-sodium Fort Union lignites can be utilized as the precursor for preparing superior powdered activated carbon (PAC) adsorbents for removal of very-high-molecular-weight-humate molecules from water (1). Activation conditions were relatively mild (750°C, 30 min) in order to limit excessive burnout during steam activation; consequently, the surface areas obtained for these carbons were relatively low (240 m^2/g for the Freedom lignite) and varied considerably depending on the lignite seam. Yet the intercept of the modified Freundlich plot (1) representing the K value for sorption of humate on the high-sodium carbon was much larger than that for the Calgon F400 carbon. The success in removing macromolecules was attributed to the larger pore structure in these carbons. Because of the high activity and low production and transportation cost, there is considerable potential for application of these low-area PACs to water treatment in the northern tier states with surface waters draining peatlands. Tests with actual surface waters from this region showed improved removal with the high-sodium carbons. Removal of these humate precursors of the disinfection by-products will enable water treatment facilities to meet newly promulgated federal drinking water regulations.

The Fort Union activated carbons were less effective, however, for adsorption of small molecules, such as hydrocarbons or chlorinated hydrocarbons, owing to the low surface areas or low number of micropores (1). Thus methods for achieving activation to larger micropore dimensions were desired to expand the potential market for the Fort Union carbons as granulated carbon. The effects of demineralizing coals on the resulting carbon properties were reported by several investigators (2–5). Since the inorganic cations in chars catalyze the gasification reaction, removal of the inorganic species resulted in slower rates and development of higher microporosity during activation. Consistent with this deactivation behavior, exchange of ammonium for sodium in the Freedom lignite prior to carbonization (under identical conditions) resulted in activated carbons with somewhat higher surface areas (BET = 350–370 m^2/g) compared to the low values of the carbon from the as-received lignite. Humate removal was less effective than with the high-sodium carbons. Toluene isotherms showed improved adsorption but were not as effective as Calgon F400.

The objective of these studies was to determine if low-cost cation removal methods evaluated earlier by Baria (6) could give lower-activity chars from the Fort Union lignites and whether more severe activation conditions could then be applied to the exchanged lignites without excessive loss of mass and loss of microporosity. The demineralization method chosen was a sulfurous acid wash that would be the most cost-effective with these lignites in removing cations.

Experimental

Preparation of Activated Carbons. Activated carbons were prepared from a high-sodium Dakota Gasification Company Freedom mine coal, ground, and sieved to 8 × 20-mesh particle size. Ion exchange was carried out by stirring the coal in 6% sulfurous acid solution overnight. The ion-exchanged coal was filtered, washed with deionized water, and air dried at 110°C. For carbonization, 50 g of the granular coal was placed in a stainless steel tube reactor and heated to 400°C in a gentle flow of nitrogen. The reactor was held at this temperature until tarry material ceased to evolve. The carbonization yield for the exchanged coal at 400°C (30 min) was 65%. For steam activation, the char was added to a quartz reactor, which was heated to the desired activation temperature in a gentle flow of nitrogen. A steam–nitrogen mixture was passed through the reactor for the desired time at the reaction temperature. The activated carbon was cooled under nitrogen and removed from the reactor, weighed, and stored under nitrogen for further use.

Carbon Properties. The steam-activated carbon was ground to −200-mesh size prior to using for water treatment. Iodine numbers were determined to investigate the effect of conditions used for generating the activated carbons on the surface area of the carbons. Isotherms were determined for solutions of trichloroethylene (TCE) (10.2 μg/mL) and toluene (10.2 μg/mL) in water by adding known weights of the carbons (1.00 to 20.00 mg) to 50 mL of the solution and stirring for 2 hr. Concentrations were determined in the equilibrated solution supernatants by extraction into minimal dichloromethane containing the internal standard fluorobenzene and gas chromatography analysis on a 3-μ DB5 phase column.

Results

Cation Removal. Lignites typically have a large content of inorganic cations (especially sodium) associated with the weak acid carboxylate groups of the organic structure. The sodium content of the Fort Union lignite ash amounts to 4%–12% as Na_2O where the ash represents 10% of the as-received weight. These cations are responsible for ash fouling during combustion and, as mentioned above, have a large effect on the gasification rate and consequently on the development of the metaplast and subsequent formation of the micropore structure. Thus dramatic effects on carbon properties and behavior are obtained by removal of these ions. The ions are removed by an exchange process, with sodium being the most easily exchanged ion. Although ammonium exchange is effective and used in analytical procedures, the use of acid is less expensive (Baria). Impure dilute sulfurous acid potentially available from flue gas represents the least costly alternative.

Washing the 16% ash (mf basis) Freedom lignite with sulfurous acid gave an ash content of 8.57% (mf basis) after drying. Thus, not only sodium, but other cations and minerals such as carbonate were removed.

Activation at Various Temperatures. The 400°C char was activated using a matrix of temperatures and activation times. The carbon yields are given in Table 1. The longer reaction times and higher temperatures gave lower carbon yields, as expected.

Activated Carbon Properties. Surface areas of the activated carbons from the exchanged lignite char are reported in Table 1. Increasing the activation temperature from 650° to 750°C resulted in increases in surface area, but further increase to 800°C gave a lower iodine number. This temperature behavior parallels that of the as-received coal, but at higher values. At 750°C, the surface areas decreased dramatically with increasing activation time. Thus optimum surface areas are obtained at 750°C for 30 min, the same conditions as with the as-received coal.

Adsorption Isotherms. To evaluate the potential for the exchanged lignite-activated carbons in PAC applications in treating

Table 1. Effect of Reaction Temperature and Time on the Carbon Yield and Surface Area (exchanged lignite char = 50 g)

Activation Conditions	Carbon Yield, %	Iodine #
Char Carbonized @400°C		179
Steam Activation @ 650°C/90 min	87	310
Steam Activation @ 700°C/90 min	83	330
Steam Activation @ 750°C/90 min	60	439
Steam Activation @ 750°C/30 min	68	483
Steam Activation @ 800°C/30 min	60	467
Steam Activation @ 750°C/60 min	64	448
Steam Activation @ 750°C/120 min	40	350
Steam Activation @ 750°C/90 min*	30	368

* = volume of steam was doubled.

halocarbon- or hydrocarbon-contaminated water, adsorption isotherms were determined for the 750° and 800°C activated carbons from the sulfurous acid-exchanged lignite in solutions of toluene and TCE in water. The isotherm data were plotted using the conventional Freundlich method (log µg removed/g sorbent versus log C_{eq} in µg/mL). The results of these plots are given in Table 2. Results from earlier tests performed with the carbons from as-received lignite and ammonium acetate-exchanged lignite (1) are also shown in Table 2. The intercepts for the isotherms of the carbons from the exchanged lignite show significant increases over those obtained for the carbon from the as-received lignite. The lower-surface-area 800°C carbon exhibits lower intercept values for toluene and TCE. Thus these intercepts, which represent the log K values for the systems, are consistent with the surface areas determined for the carbons. The 750°C conditions optimize both the surface area and adsorption potential. The intercept for the 750°C carbon from sulfurous acid-washed lignite was also improved over that observed earlier for the 750°C carbon from ammonium acetate-exchanged lignite.

Table 2. Isotherm Data for Activated Carbons from Lignite

Activated Carbon		Toluene		TCE	
Lignite	Act. Temp.	Intercept	Slope	Intercept	Slope
Freedom – H_2SO_3	750°C	4.69	0.25	4.66	0.29
Freedom – H_2SO_3	800°C	4.09	0.48	3.27	1.47
Freedom – NH_4^+ Ac	750°C	4.30	0.59		
Freedom – a.r.	750°C	3.00	1.17		

Conclusions

The sulfurous acid wash appears to be more effective than the ammonium exchange in removing organically associated cations that can catalyze excessive burnout during activation and perhaps other minerals, such as calcium carbonate, that may plug pores. Activation of the sulfurous acid-exchanged lignite resulted in higher surface areas, owing to development of microporosity in the carbon. Higher activation temperatures resulted in lower surface area, which may be attributed to the very high reactivity of the char, even in the absence of the cations. Thus surface areas are lower than those attainable from bituminous coals. Removal of toluene and TCE representing small hydrocarbon and halocarbon molecules was improved by the exchange procedure.

Acknowledgment. This research was done with the support of the U.S. Department of Energy (DOE) National Energy Technology Laboratory Cooperative Agreement No. DE-FC26-98FT40320. However, any opinions, findings, conclusions, or recommendations expressed herein are those of the authors and do not necessarily reflect the views of DOE.

References

(1) Olson, E.S.; Sharma, R.K.; Eylands, K.E.; Stepan, D.J. *Fuel Chem. Div. Preprints* **2002**, *47(2)*, 472.
(2) Samaras, P.; Diamadopoulas, E.; Sakellaropoulos, G.P *Carbon* **1994**, *32*, 771.
(3) Mahajan, O.M.; Walker, P.L., Jr. *Fuel* **1979**, *58*, 333.
(4) Calahorro, C.V.; Cano, T.C.; Serrano, V.G. *Fuel* **1987**, *66*, 479.
(5) Serio, M.A.; Solomon, P.R.; Bassilakis, R. *Proceedings of International Conference on Coal Science* 1989, 341.
(6) Baria, D.N. *Proceedings of the Third Annual Pittsburgh Coal Conf.* Pittsburgh, PA, 1986, 71.

DEVELOPMENT OF MICROPOROUS ACTIVATED CARBONS FROM UNBURNED CARBON IN FLY ASH

Yinzhi Zhang, Zhong Tang, M. Mercedes Maroto-Valer and John M. Andrésen

The Energy Institute and the Department of Energy and Geo-Environmental Engineering,
The Pennsylvania State University,
405 Academic Activities, University Park, PA 16802, USA

1. Introduction

Due to the widely application of low-NO_x burner technologies, fly ashes of high unburned carbon content derived from coal-fired combustors are an increasing problem for the utility industry [1]. High carbon content fly ashes cannot be marketed as a cement extender[2], and therefore, have to be disposed. In 1999, over 60 million tons of fly ash and around 6 million tons of fly ash carbon were generated by the utility coal industry [3]. The authors have previously conducted extensive studies on the characterization of unburned carbon and showed the potential to produce activated carbons from unburned carbon by a one-step steam activation process [4,5]. However, the unburned carbon in fly ash has gone through a devolatilization process while in the combustor at temperatures above 1200°C that are much higher than those conventionally used for devolatilization or carbonization of precursors of activated carbons. Therefore, the reactivity of fly ash carbons during the activation process is relatively low and the activated carbons produced from fly ash carbon by one-step activation have a high content of mesopores[6]. Accordingly, the present study focuses on the modification of the one-step activation process in order to promote the development of microporosity, which is highly desired in commercial activated carbon. Nitric acid and hot air are widely used to modify the surface of carbon solids[7-9]. Accordingly, in this study nitric acid and hot air were selected to pre-oxidize the fly ash carbon prior to activation in order to produce activated carbon with comparable properties to those reported for commercial activated carbons.

2. Experimental

2.1 Samples. The parent study sample, FA-1, was collected at Penn State University from a 2 MM Btu/hour pulverized coal-fired suspension firing research boiler that uses a high volatile bituminous coal from the Middle Kittanning seam. Two pretreatment methods were developed, where the first one involves oxidizing the fly ash carbon in boiling nitric acid. Prior to the nitric treatment, the unburned carbon was enriched by flotation/sink and acid ($HCl/HNO_3/HF$) digestion at 65°C. The carbon content of the sample after demineralization is higher than 97%. The resulting samples after nitric acid oxidation were named as FA1-NX, with X representing the nitric acid oxidation time (in hours). The activation of the pretreated samples was carried out in a fixed bed reactor that was placed inside a horizontal furnace. The resulting activated carbons were designated as FA1-NX-851, with X representing the hours of nitric acid pretreatment and 851 representing activation at 850°C for 1 hour. For the second pretreatment method, the fly ash sample was oxidized in air for different time periods. The resultant activated carbons were designated as FA1-GPX-851, with X representing the number of hours pretreated in air. The activation experiments for the air pretreated samples were carried out in a fluidized bed reactor that was placed inside a vertical furnace, as previously described [5]. For the purpose of comparison, the untreated samples were also activated under the same conditions.

2.2 Characterization. A Kratos Analytical Axis Ultra XPS was used to study the surface chemistry of the samples. XPS quantification was performed by applying the appropriate relative sensitivity factors (RSFs) for the Kratos instrument to the integrated peak areas. The approximate sampling depth under these conditions is 25Å. The porosity of the samples was characterized by conducting standard N_2 adsorption isotherms at 77K using a Quantachrome adsorption apparatus, Autosorb-1 Model ASIT. The pore sizes 2nm and 50nm were taken as the limits between micro- and mesopores, and meso- and macropores, respectively, following the IUPAC nomenclature [10].

3. Results and Discussion

3.1 Nitric acid pretreatment. As expected, nitric acid pretreatment successfully introduced oxygen surface groups on the fly ash carbon, as showed by the XPS data presented in Table 1. The sample FA1 prior to nitric acid treatment already contains 10.5% oxygen on the surface, probably due to oxygen introduced by the acid digestion process ($HCl/HNO_3/HF$). With increasing oxidation time, the oxygen content on the surface of the fly ash carbon increases, and when the pretreatment time is extended to 5 hours, the surface oxygen content of the fly ash carbon is as high as 16.7%. Species observed on the surface of the samples include C-C, C-(O, N) and COO^-. All the pretreated samples contain distinct COO^- bands at 288.5eV. A smaller, unresolved C-(O, N) peak might also have been present. A curve fit to the experimental carbon 1s spectra showed that the nitric acid pretreatment created a large amount of carboxylic COO- groups on the surface of the fly ash carbon, as previously reported for oxidation of anthracites [9].

Table 1. Summary of Elements Detected by XPS (Rel. Atom %)

Sample	C	O	Others*
FA1	81.3	10.5	8.2
FA1-N1	84.8	14.6	0.6
FA1-N3	84.5	14.0	1.5
FA1-N5	82.5	16.7	0.8

* Includes halogen, nitrogen, and earth mineral elements.

The porous texture properties, as determined from the 77K N_2-isotherms, of the parent sample and its counterparts oxidized with nitric acid are presented in Table 2. It can be seen that the nitric acid pretreatment increased the porosity of the fly ash carbon. For example, the surface area of the fly ash carbon increases to $278 m^2/g$ for 5 hours pretreatment compared to $125 m^2/g$ for the parent sample. The average pore size decreases to 2.21 nm from 2.46 nm, which indicates that the pores developed during pretreatment are mainly micropores.

Table 2. Porous texture characteristics of the parent sample and its counterparts oxidized with nitric acid.

Sample	BET surface area, m^2/g	Pore volume, ml/g	Average pore diameter, nm
FA1	125	0.077	2.46
FA1-N3	179	0.104	2.34
FA1-N5	278	0.153	2.21

3.2 Activation of nitric acid pretreated samples. The samples pretreated with nitric acid were then activated by steam at 850°C for 1 hour. The N_2-77K isotherms of the resultant activated samples (FA1-N1-851, FA1-N3-851, and FA1-N5-851) are shown in Figure 1, and Table 3 lists the surface area and pore volumes calculated from the isotherms. For the purpose of comparison, the sample without pretreatment (FA1-851B) is also included in Figure 1 and

Table 3. The isotherms of all the pretreated samples have higher adsorbed volumes than the sample without pretreatment (Figure 1). For the 1 hour pretreatment sample (FA1-N1-851), the isotherm has similar shape to the sample without pretreatment, but it has a larger adsorbed volume for the micropore filling. For the 3 and 5 hours pretreatment samples (FA1-N3-851 and FA1-N5-851), the micropore filling at low relative pressure has not changed significantly, except than the isotherms present a more open knee, indicating a wider micropore size distribution.

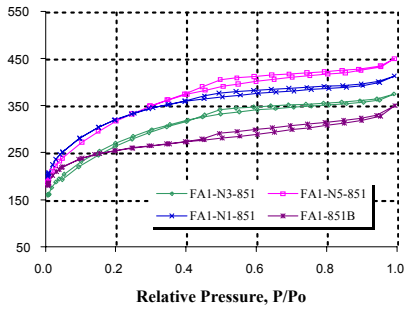

Figure 1. N_2-77K isotherms of the activated parent sample and the samples activated after nitric acid pretreatment.

Table 3 shows that after 1 hour pretreatment, the surface area of the resultant activated carbon is as high as 1139m^2/g, compared to 890m^2/g for the sample without pretreatment. Similarly, the pretreated sample has a smaller average pore size, 2.16nm, compared to 2.27nm for the sample without pretreatment. This activated sample also has a micropore surface area of 1053m^2/g. With longer pretreatment time, the surface area decreases together with a larger average pore size. Therefore, for the nitric pretreatment, the optimal pretreatment time is 1 hour.

Table 3. Porous Texture Characteristics of the Activated Parent Sample and the Samples Activated after Nitric Acid pretreatment.

Sample	BET surface area, m^2/g	Pore volume, ml/g	Average pore diameter, nm
FA1-851B	890	0.505	2.27
FA1-N1-851	1139	0.615	2.16
FA1-N3-851	1131	0.666	2.36
FA1-N5-851	969	0.558	2.30

3.3 Activation of air treated samples. The samples were pretreated for 1-3 hours in hot air and then steam activated at 850°C for 1 hour. Table 4 presents the porous texture characteristics of the samples activated after air pretreatment (FA1-GP-1, FA1-GP-2, and FA1-GP-3) and the parent sample (FA1-851).

Table 4. Porous Texture Characteristics of the Parent Sample (FA1-851) and Samples Activated After Air Pretreatment (FA1-GP-1, FA1-GP-2, and FA1-GP-3).

Sample	BET surface area, m^2/g	Pore volume, ml/g	Average pore diameter, nm
FA1-851	585	0.326	2.23
FA1-GP-1	732	0.434	2.37
FA1-GP-2	931	0.526	2.26
FA1-GP-3	892	0.546	2.45

When comparing the two samples activated without pretreatment (FA1-851 and FA1-851B), FA1-851 has a much smaller surface area, 585m^2/g (Table 4) than that reported for FA1-851B, 890m^2/g (Table 3). Although both samples were activated at the same temperature and for the same period of time, FA1-851B was obtained from the FA1 fly ash carbon after acid digestion under 65°C, while FA1-851 was obtained directly from FA1 without the acid digestion step. As discussed in Section 3.1, the acid digestion process introduced some oxygen, which will probably improve the reactivity of the sample during activation. Furthermore, for FA1-851 and FA1-851B different reactor designs and operation conditions were used, where FA1-851 was activated under fixed bed conditions, while FA1-851B was activated in a fluidized bed. The data in Table 4 show that the pretreated samples present surface areas up to 59% larger than their untreated counterpart (931 m^2/g with 2 hour pretreatment compared to 585m^2/g without pretreatment). When extending the pretreatment time to 2 hours, the surface area and pore volume for the resultant activated carbon increase to 931m^2/g and 0.526ml/g, respectively, together with an average pore size of 2.26nm. However, extending the pretreatment time to 3 hours resulted in a decrease of the surface area and pore volume.

4. CONCLUSIONS

The two pretreatment methods used here have increased the surface area and pore volume compared to the samples without pretreatment. The results reported here show that both methods are effective to increase the surface area of the resultant activated carbon, especially the micropore volume. The resultant activated carbons have a surface area up to 1139m^2/g (including micropore surface area 1053m^2/g), and pore volume 0.615ml/g (including micropore volume 0.518ml/g). The properties of the produced activated samples will be compared to commercial activated carbons.

ACKNOWLEDGEMENTS

The authors wish to thank the Consortium for Premium Carbon Products from Coal (CPCPC) at The Pennsylvania State University for financial support.

REFERENCES

(1) Tyson, S. S. Unintended effects of NOx emissions control strategies on unburned carbon and CCP marketability, Proceedings of 3rd annual conference on unburned carbon on utility fly ash, 1997, Pittsburgh, 3-5

(2) Hill, R. L.; Sarkar, S. L.; Rathbone, R. F. and Hower J.C. Cement and Concrete Research, 1997, 27(2), 193-204

(3) Zhang, Y.; Maroto-Valer, M.M; Lu, Z.; Andresen, J.M. and Schobert, H.H. Potential non-fuel uses of unburned carbon from fly ash for value added carbon products. Proceedings of 18th annual international Pittsburgh coal conference, 2001, New South Wales, Australia.

(4) Maroto-Valer, M.M.; Taulbee, D.N. and Hower, J.C. Novel separation of the differing forms of unburned carbon present in fly ash using density gradient centrifugation, Energy & Fuels, 1999, 13, 947-953

(5) Zhang, Y.; Maroto-Valer, M.M.; Lu Z.; Andrésen, J.M. and Schobert, H.H. One step activation of coal combustion waste, Proceedings of American carbon society Carbon'01 conference, 2001, CD-ROM Zhang38.1.pdf.

(6) Zhang, Y.; Lu, Z.; Maroto-Valer, M.M.; Andrésen, J.M. and Schobert, H.H. Comparison of high unburned carbon fly ashes from different combustor types and their steam activated products, submitted to Energy & Fuel.

(7) Stoekli, F. and Huguenin, D, Pretreatment and physical activation of acetylene cokes, Fuel, 1994, 73, 1929-1930

(8) Lee. S. H. and Lee, C.D., Influence of pretreatment and activation conditions in the preparation of activated carbons from anthracite, Korean J. Chem. Eng., 2001, 18(1), 26-32.

(9) Serrano-Talavera, B.; Muñoz-Guillena, M.J.; Linares-Solano, A.L. and Salinas-Martînez de Lecea, C. Activated carbons from Spanish coals. 3. Preoxidation effect on anthracite activation, Energy & Fuels, 1997, 11, 785-791

(10) Sing, K.S.W.; Everett, D.H.; Haul, R.A.W. and et al, Reporting physisorption data for gas/solid systems with special reference to the determination of surface area and porosity, Pure & Appl. Chem., 1985, 57(4), 603-609

FORMATION OF CRYSTAL STRUCTURES DURING ACTIVATED CARBON PRODUCTION FROM TURKISH ELBISTAN LIGNITE

Sevil Çetinkaya[1], Billur Sakintuna[2] and Yuda Yürüm[2]

[1]Department of Chemistry,
Hacettepe University,
Beytepe, Ankara 06532, Turkey
[2]Facuty of Engineering and Natural Sciences, Sabanci University,
Tuzla, Istanbul 34956, Turkey

Abstract

In this study, activated carbons were produced from raw, HCl treated and HCl/HF treated (demineralized) Elbistan lignites under various experimental conditions. In carbonization experiments, coals were heated to four different temperatures 700°C, 800°C, 900°C, and 1000°C with a heating rate of 10°C/min, under a nitrogen flow of 100 ml/min for two hours. In activation experiments, coals were first carbonized as described and then activated in carbon dioxide atmosphere at the final carbonization temperature for an additional two hour. The flow rate of pure carbon dioxide was held at 100 ml/min. The BET surface area of the lignite was measured as 3.7 m^2. The highest surface area was measured for the HCl-HF treated sample activated at 1000°C as 1177.6 m^2. Scanning tunnelling microscopy was used to analyze surfaces of carbonized and activated coal samples. X-ray diffractograms indicated the presence of some crystalline carbon structures in the products of carbonization and activation reactions.

Introduction

The problem of environmental protection is continually increasing the importance of treatment of wastewater and gas emissions in order to remove toxic substances. This has renewed interest in the production of activated carbons. Continous increase in demand makes it necessary to make use of different basic materials. Among these, coal is the most widely used so that about 60% of the activated carbon production is obtained from this source [1]. Both high and low rank coals are used for the production of activated carbons [2]. At the same time, activated carbon is manufactured from various raw materials such as peat, polymeric resins, wood and coconut shells [3-6]. The effecting factors for the production of activated carbons are: initial material (used for manufacturing), the heat treatment conditions, reagent gas, residence time, inorganic impurities [7-9].

The total porous structure of an activated carbon is formed by a wide range of pore sizes. The macropores of an activated carbon act as transport pores, enabling the molecules of the adsorptive to reach the smaller pores situated in the interior of the carbon particle. Thus, the macropores are not important from the point of view of the amount adsorbed in them, since their surface area is very low, but they affect the rate of diffusion into the meso and micropores. The micropores constitue the largest part of the internal surface and consequently, most of the adsorption takes places within them; at least 90% of the total surface area of an activated carbon corresponds to the micropores. The mesopores, which branch off from the macropores, serve as passages to the micropores for the adsorptive besides acting as pores where capillary condensation can take place.

The two main steps in the production of the activated carbon are carbonization and activation. The first step is carbonization and is usually performed in an inert atmosphere to remove volatile matter. The coal structure decomposes by the breakage of the least stable bonds within the structure which are methylene , oxygen, and sulfur-bridges between the aromatic building blocks [10]. The char is enriched in carbon and more aromatic in comparison with the raw coal particle. The latter step of activation consist of mild oxidation with such oxidizing gases as steam, CO_2 and air to develop an appropriate pore structure [11].

The aim of this study was the preparation of activated carbons from a low rank lignite. Effect of carbonization and activation temperatures, influence of the mineral matter content of the coal used on the properties os carbons produced were investigated. Changes in surface area, surface structures and crystal structures developed during carbonization and activation were also investigated.

Experimental

Materials

Elbistan lignite was used in this study. Lignite samples were ground and sieved to a particle size less than 100 μm. Proximate and ultimate analyses of the materials are shown in Table1. There are three main steps as demineralization, carbonization and activation of samples at different temperatures during production of activated carbons from materials. To compare the effect of mineral matter on carbonization and activation experiments, the acid treatment was carried out by washing the coal with HCl followed by HF. 18.0 g coal sample was mixtured for 1 hour in 120 ml 5 N HCl solution. Then the treated coal washed in water with warm distilled water. Washed coal was mixtured with 120 ml 22 N HF for 1 hour. The coal was filtered off and washed. Treated (HCl and HF) coals dried at 100°C in an inert atmosphere.

Carbonization Experiments

Raw, HCl and HCl-HF treated coal samples were dried at 100°C an inert atmosphere. 8.00 g sample was placed into a porcelain crucible and then dropped into a furnace purged with ultra high pure nitrogen. Coal samples were heated to four different temperatures 700, 800, 900 and 1000°C with a heating rate of 10°C/min, under a nitrogen flow of 100 ml/min for two hours. After the carbonization experiments, system was cooled to room temperature under the nitrogen flow. Chars were taken out from the system.

Activation Experiments

Carbonized coals were activated under a CO_2 flow of 100 ml/min at the final carbonization temperature for an additional two hours. System was cooled to room temperature under the nitrogen flow. After that, chars were taken out from the system. Chars obtained from carbonization and activation experiments stored for physical characterization tests.

Surface Analysis

Surface areas of activated carbons were determined by ASAP2000 Accelerated Surface Area and Porosimetry system manufactured by Micromeritics Co., USA. Surface area of the samples were determined by using BET equation in the relative pressure range of between 0.05 to 0.25, over five adsorption points.

Scanning Tunnelling Microscopy Studies

A scanning tunnelling microscope which was designed and constructed in our laboratories was used to obtain the images of the coal surfaces. All STM measurements were performed in air at room temperature. The STM was operated at a variable current mode with Pt/Ir sharp tip, with an average tunneling current of 0.5 nA and with a bias voltage in the range of 250-500 mV. Median and Lowpass Filters were used to reduce the noise from the environment and recover the background.

X-Ray Diffraction Measurements

X-ray diffractograms of the samples of carbonized and activated products were measured with a Bruker axs advance powder

diffractometer fitted with a Siemens X-ray gun and equipped with Bruker axs Diffrac PLUS software. The sample was rotated (15 rpm) and swept from 2q = 10º through to 90º using default parameters of the program. The X-ray generator was set to 40kV at 40 mA.

Results and Discussion

The aim of this study was to investigate the effects of acid treatments and temperature on the pore structure of the coal char after the carbonization and activation processes. Nitrogen gas adsorption measurements of raw Elbistan lignite, carbonized and activated lignite were given in Table 2. The BET surface area for raw Elbistan lignite was found as 3.7 m^2/g. Surface areas of HCl and HCl-HF treated lignite samples were measured as 3.8 m^2/g and 2.5 m^2/g, respectively. Treatment with HCl dissolved minerals which were soluble in HCl such as carbonates, silicates, etc. and treatment with HCl-HF eliminated all mineral matters except pyrite. The changes in BET surface areas were due to the removal of inorganic matter which generated high surface area and developed micropores. When the raw and demineralized lignites were carbonized at 700°C, surface areas of chars obtained from carbonization processes increased enormously. The rapid increase in the surface area was attributed to the widening of existing pores or the creation of new pores. As shown in Table 2, surface area of carbonized char (340.4 m^2/g) produced from HCl-HF demineralized lignite greater than those produced from raw and HCl treated lignite (147.6 m^2/g and 243.6 m^2/g). The char obtained from HCl-HF treated lignite at 700°C possessed the higher adsorption capacity than raw and HCl treated chars. It showed that more micro or macropores developed in this sample at 700°C than for the raw and HCl treated lignite and HCl-HF treatment increased the accessible micropores. The similar trends were found at 800°C, 900°C and 1000°C. Surface areas of carbonized chars obtained from HCl-HF treated samples were found to be much higher than those obtained from untreated and HCl treated lignite samples. Surface areas of chars prepared under carbonization at 800°C for raw, HCl and HCl-HF treated samples were 170.8 m^2/g, 254.0 m^2/g and 395.9 m^2/g. The further activation with CO_2, after carbonization, increased the surface area of these samples and changed the surface area of activated chars to 201.3 m^2/g, 283.5 m^2/g and 494.0 m^2/g, respectively.

The variation of carbonization and activation temperature affected the surface area of chars obtained after these processes. Surface areas of carbonized samples obtained at 800°C were greater than that of at 700°C. The increase of the surface areas from 147.6 to 170.8, from 243.6 m^2/g to 254.0 m^2/g, from 340.4 m^2/g to 395.9 m^2/g by increasing the temperature of carbonization from 700°C to 800°C was explained with the loss of volatile matter which leads to development of porosity. So surface areas of chars increased as the carbonization temperature increased. Similar trends were determined in the activated chars. The surface characteristics of the activated carbons were influenced by the activation temperature. The char obtained from activation at 1000°C from HCl-HF treated lignites has the biggest area.

X-ray diffractograms indicated the presence of crystalline carbon structures in the products of carbonization and activation reactions.

Table 1. Proximate and Ultimate Analysis of Elbistan Lignite

Proximate analysis	**%, dry**
Volatiles	44.8
Fixed Carbon	20.9
Ash	34.3
Ultimate Analysis	**%, dmmf**
C	53.0
H	5.8
N	1.8
S	3.6
O (by difference)	35.8

Table 2. BET Surface Areas of Carbonized and Activated Lignite Samples

Sample	**BET Area (m^2/g)**
Raw	3.7
HCl treated	3.8
HCl-HF treated	2.5
Raw- 700°C carbonized	147.6
HCl treated- 700°C carbonized	243.6
HCl-HF treated- 700°C carbonized	340.4
Raw- 700°C activated	213.8
HCl treated- 700°C activated	257.2
HCl-HF treated- 700°C activated	440.5
Raw- 800°C carbonized	170.8
HCl treated- 800°C carbonized	254.0
HCl-HF treated- 800°C carbonized	395.9
Raw- 800°C activated	201.3
HCl treated- 800°C activated	283.5
HCl-HF treated- 800°C activated	494.0
Raw- 900°C carbonized	182.5
HCl treated- 900°C carbonized	328.8
HCl-HF treated- 900°C carbonized	527.9
Raw- 900°C activated	71.5
HCl treated- 900°C activated	377.7
HCl-HF treated- 900°C activated	675.0
Raw- 1000°C carbonized	135.0
HCl treated- 1000°C carbonized	413.9
HCl-HF treated- 1000°C carbonized	562.4
Raw- 1000°C activated	20.9
HCl treated- 1000°C activated	437.2
HCl-HF treated- 1000°C activated	1177.6

References

(1) Wilson J.; *Fuel* **1981,** *60*, 823.
(2) Samaras P.; Diamadopoulos E.; Sakellaropoulas P.; *Carbon* **1991**, *29*, 1181.
(3) Hashimoto K.; Miura K.; Yashikawa F.; Pajares J.A.; *Fuel Process. Tech.* **1993**, *33*, 333.
(4) Rodriguez-Reinoso F.; Lopez-Gonzalez J.; Berenguer C.; *Carbon* **1982**, *20*, 513.
(5) Derbyshire, F.; McEnaney, B.; *Energia* **1991**, *2*, 1.
(6) Clements, A.H.; Matheson, T.W.; Rogers, D.E.; *Fuel* **1991**, *70*, 215.
(7) Wiagmans T.; *Carbon* **1989**, *27*, 13.
(8) Gomez M.J.I.; Garcia A.G.; Martinez de Lecea C.S.; Solano A.L.; *Energy and Fuels* **1996**, *10*, 1108.
(9) Vyaz S.N.; Patwardhan S.R.; Vijayalaksmi S.; Gangadhar B.; *Fuel* **1993**, *72*, 551.
(10) Tromp, J.J.P; Moulijn J.; in New Trends in Coal Science; Yürüm Y., Ed.; NATO ASI Series, 1988, *244*, pp. 305-331.
(11) Rist L.P.; Harrison D.P.; *Fuel* **1985**, *64*, 291.

EFFECT OF OXIDATIVE RESISTANT HYDROGEN DONORS FROM AROMATIC LIQUIDS TOWARDS REDUCED AUTOXIDATIVE AND PYROLYTIC DEPOSITIONS IN THERMALLY STRESSED JET FUEL

John M. Andresen, James J. Strohm and Chunshan Song

The Energy Institute, The Pennsylvania State University,
209 Academic Projects Bldg., University Park, PA 16802, USA

Introduction

In future high-Mach jet aircraft the jet fuel is expected to experience temperatures as high as 480°C (900°F) or above due to its dual role as a coolant for the mechanical and electrical parts of the aircraft (1). Coal-based liquids that are rich in naphthalenes have shown great potential to be transferred into additives for advanced jet fuels that meet the more stringent thermal stability requirements under pyrolytic conditions (2). An additional problem with jet fuels is the presence of dissolved oxygen (from air), which reacts with the fuel in the autoxidative regime (150-250°C) before the fuel and its oxygenated reaction products enter the pyrolytic regime (400-500°C) (3, 4). Oxygen substituted antioxidants are added to the fuel to prevent gum formations in the autoxidative regime while hydrogen donors can be used to prevent thermal degradation of the jet fuel by capturing free radicals generated by pyrolytic cracking of the paraffinic compounds (5, 6). However, traditional antioxidants may not prevent hydrogen donors from interacting with oxygen in the pyrolytic regime thus reducing the thermal stability of the jet fuel by prohibiting the hydrogen donors from stopping the free radical propagation reactions leading to solid deposits (7).

Oxygen substituted hydrogen donors that can be derived from coal liquids, including α-tetralone and α-tetralol, could increased thermal performance of jet fuels both in the pyrolytic and oxidative regime. Scheme 1 outlines one such route and suggests that the utilization of coal derived chemicals can be the key in reaching the thermal stability requirements for future high-Mach jet aircrafts.

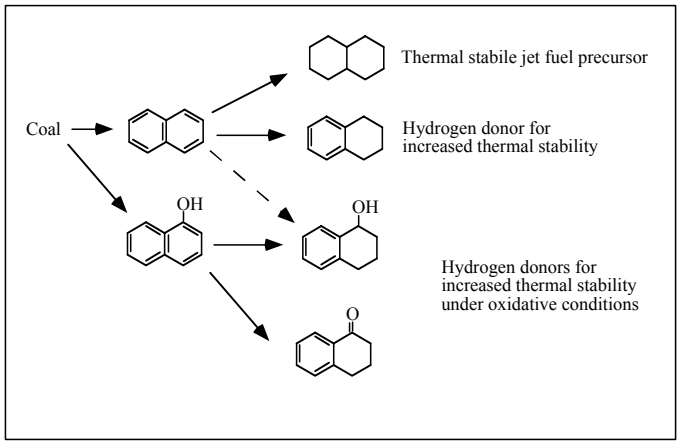

Scheme 1. Possible utilization of coal derived chemicals as a key element in reaching the thermal stability requirements for future high-Mach jet aircrafts.

Firstly, naphthalene is readily obtained from coal. It can then either be fully hydro-treated to decahydronaphthalene and serve as a precursor for thermal stabile jet fuel in itself, or be partially hydro-treated over to hydrogen donors, i.e. tetralin. Further, coal-derived naphthols can be partially hydrogenated to α-tetralone or α-tetralol (8), which may improve the oxidation-resistance both of the fuels and the hydrogen donors derived from coal. Accordingly, this study has investigated the above coal-derived chemicals as benign thermal stabilizers for jet fuels using flow-reactor tests, where the thermal stressing of the high performance liquids was closely related to the actual operational conditions under both non-oxidative and oxidative conditions. Significant improvements in the ability of these modified hydrogen donors to withstand interaction with oxygen dissolved in the jet fuel were observed.

Experimental

The jet fuel studied was JP-8 that is similar to the commercial jet fuel Jet-A. The hydrogen donors tested were α-tetralone (Aldrich, 98%) and α-tetralol (Acros, 97%). For the flow reactor studies the charge tank was purged with high purity O_2 (99.5%) for the autoxidative studies and high purity N_2 (99.995) for the pyrolytic experiments. A liquid hourly space velocity (LHSV) of 450 was used. A silcosteel tubing was used to avoid secondary surface reactions and the maximum bulk liquid fuel temperature at the exit of the furnace was measured by a stripped thermocouple inserted into the tube. The GC/MS traces were reported according to this exit temperature. The GC/MS analysis was conducted on the liquid products using a Shimadzu GC-174 coupled with a Shimadzu QP-5000 MS detector. The column used was a Restek XTI5 column with a coating phase of 5% diphenyl / 95% dimethyl polysiloxane and was heated from 40 to 290°C with a heating rate of 6°C min^{-1}. The carbon deposit analyses were carried out using a LECO RC 142 multiphase carbon analyzer on 2 cm pieces of the flow reactor tubing.

Results and Discussion

Figure 1 shows the GC/MS traces of JP-8 prior to stressing (bottom), stressed under O_2 at 772°C for 3 hr without addition of hydrogen donors (middle), and with addition of candidates for coal-derived hydrogen donors (top). When stressed without hydrogen donors there is a significant production of aromatic compounds and a tremendous reduction in the paraffinic content for the JP-8. Accordingly there is a significant boost in the thermal stability of the jet fuel JP-8 when a mixture of the hydrogen donors α-tetralone and tetralin was added to the jet fuel as shown from the GC/MS traces in Figure 1. The addition of α-tetralone seems to reduce the impact of oxygen on the JP-8 and also to enhance the overall performance of the tetralin added.

Further, the hydrogen donors inhibit the formation of 3 and 4 ring aromatic compounds that are clearly present for the JP-8 stressed alone (Figure 1). These compounds are mainly associated with the formation of solid deposit (3). This is also illustrated in Figure 2 where the solid deposit along the fuel line is compared. The initial length at 8 cm corresponds to the inlet temperature around 25°C. The first peak at 25 cm indicates autoxidative deposition while the deposit above 50 cm derives from pyrolytic deposit. Clearly for the JP-8 stressed alone there is a significant formation of deposit in both the autoxidative and pyrolytic regimes. The combination of α-tetralone and tetralin clearly helped preventing both deposition of oxygenated compounds as well as solid deposit at higher temperatures.

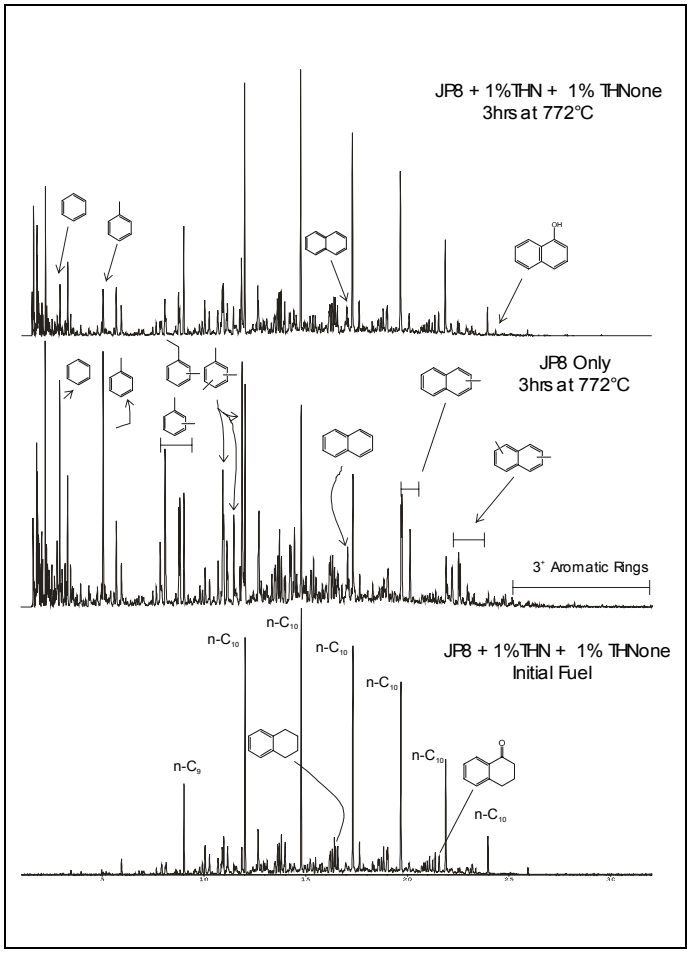

Figure 1. Comparison of GC/MS traces for JP-8 prior to stressing (bottom), stressed under O_2 at 772°C for 3 hr without addition of hydrogen donors (middle), and with addition of candidates for coal-derived hydrogen donors (top).

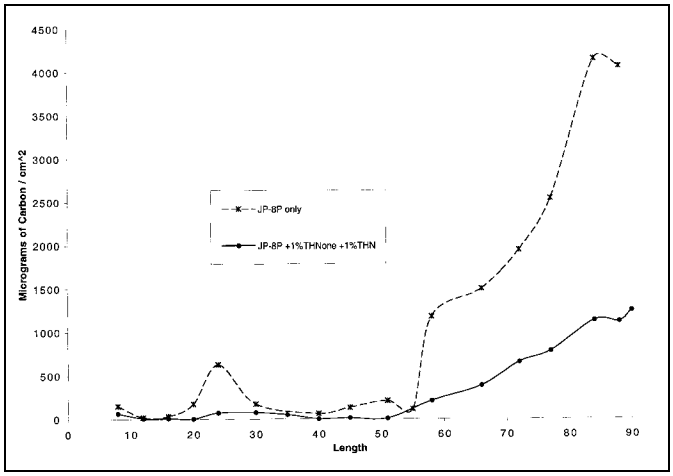

Figure 2. Comparison of the solid deposit along the fuel line for JP8 with and without hybrid donor stressed at 772C for 3 hrs in a flow reactor under oxygen.

Conclusions

The use of oxygenated hydrogen donors, such as α-tetralone, significantly increased the thermal stability of the jet fuel JP-8 under oxidative conditions. Further, the mixture of the hydrogen donors α-tetralone and tetralin suppressed the formation of aromatic compounds during stressing of the jet fuel JP-8, especially 3 and 4 ring aromatics. In addition, the use of α-tetralone and tetralin reduced both the autoxidative and pyrolytic solid deposition from the JP-8 jet fuel in the fuel lines studied.

Acknowledgement. The authors wish to thank the U.S. Air Force Office of Scientific Research for financial support. We are grateful to Prof. Harold H. Schobert form Penn State and to Mr. William Harrison, Dr. Cindy Obringer and Dr. Tim Edwards of the U.S. Air Force Wright Laboratory for helpful discussions.

References

(1) Edwards, T., Prepr. - Am. Chem. Soc. Div. Petrol. Chem. 1996, 41(2), 481.
(2) Song, C.; Eser, S.; Schobert, H.H.; Hatcher, P.G., Energy & Fuels 1993, 7, 234.
(3) Andresen, J.M.; Strohm, J.J.; Sun, L.; Song, C., Energy & Fuels 2001, 15, 714.
(4) Song, C.; Eser, S.; Schobert, H.H.; Hatcher, P.G., Energy & Fuels 1993, 7, 234.
(5) Hazlett, R.N., Thermal Oxidative Stability of Aviation Turbine Fuels, ASTM, Philadelphia, PA; 1991.
(6) Andresen, J.M.; Strohm, J.J.; Coleman, M.M.; Song, C. Prepr. - Am. Chem. Soc., Div. Fuel Chem. 2000, 45(3), 454.
(7) Strohm, J.J.; Andresen, J.M.; Song, C., Prepr. - Am. Chem. Soc., Div. Fuel Chem. 2001, 46(2), 487.
(8) Shao, J.; Holtzer, G.; Song, C., Prepr. - Am. Chem. Soc. Div. Petr. Chem. 2000, 45(1), 18.

EFFICACY OF COAL-BASED ACID ON THE BIOACTIVITY OF TRIBENURON-METHYL

Caifeng Zhang[1,2], Shanxiang Li[1], Baoqing Li[1] and Wen Li[1]

1 State Key Lab of Coal Conversion, Institute of Coal Chemistry, Chinese Academy of Sciences, P. O. B. 165, Taiyuan, 030001, P.R. China
2 Department of Chemistry, Taiyuan Normal College, Houjiaxiang, Taiyuan, 030001, P.R. China

Introduction

Pesticide plays an important role in agriculture. It was reported that the loss made by insect, plant disease and weed occupied 10% ~ 15% of the total agricultural product but the pesticide can save 15%~30% of the loss. However, the application of the pesticide brought about many serious side effects such as environmental pollution and harmfulness to human and animal. Nowadays, research on the pesticide is focused on exploring the method decreasing the usage and harm of pesticide.

Many studies have proved that the pesticides in soil and water may interact with humic substances (HS), the most widespread and ubiquitous natural non-living organic materials occurring in all terrestrial and aquatic environments from the end products of chemical and biological degradation of plant residues[1,2]. The interaction affected degradation and detoxication of the pesticides, residue persistence and monitoring, mobilization and transport, bioavailability and phytotoxicity, and bioaccumulation[3,4,5,6]. In general, the modes of interaction include adsorption, partitioning and solubilization, catalysis and dealkylation, and photosensitization[7]. HS is well recognized and widely applied as fertilizer and growth plant regulator. Patents reported that humic acid was used as adjuvants for slow-release pesticide compositions when pesticides were added into fertilizer with humic substances[8,9]. Our patents showed that coal-based acid enhanced the bioactivity of fungicide and insecticide[10,11].

Tribenuron-methyl is Sulfonylurea herbicide against two-leaf weed with the advantage of the best bioactivity as yet. But it is clear that the Sulfonylurea led to resistance to pesticide when the herbicide was used continuously. The surface adjuvant can improve the bioactivity of tribenuron-methyl.

Coal-based acid (CA) is the humic substance resulted from coal. There are two kinds of water-soluble coal-based acid (WSCA): (1) originally existed in coal, and (2) newly formed through oxidation-degradation of coal. This work studied the adjuvant effect of the two kinds of WSCA on the bioactivity of tribenuron-methyl.

Experimental

Preparation of WSCA. W-WSCA was prepared by the following procedures. Wuchuan weathered lignite was oxidized and dissociated by HNO_3 with Zn as catalyst for 2h, in which the ratio of solid and liquid was adjusted to 1:2~1:4 by water. After the first product was alkalized by NaOH for 2h at 80~100°C, the degradation was performed using H_2SO_4, and pH value of the product was further adjusted to 4~6 by HNO_3. Finally, the liquid of the product was separated by precipitation and dried with infrared lamp at 70°C to get W-WSCA. H-WSCA was prepared using Huolinhe lignite by the same procedure as that of W-WSCA. Jincheng weathered coal mixed with 10 times water was stirred and the mud was poured, the residue was precipitated for 0.5~1 h. The residue was added with 10 times water again and its pH value was adjusted to 1.2~1.5 by H_2SO_4, and then extracted for 1~2 h in water bath at 60~70°C. Finally, the liquid was separated and dried with infrared lamp at 70°C. The product was purified further with acetone to get J-WSCA.

The content and functional groups of WSCA were determined with the method described by Schnitzer and Khan[12].

Tribenuron-methyl. The commercial formulation of tribenuron-methyl (content: 75% DF) produced by E. I. du Pont de Nemours and Company.

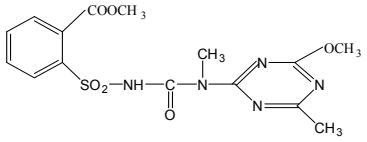

Figure 1 The chemical structure of tribenuron-methyl (T)

Instrumentation. An EA1108 elemental analyzer (Carlo Erba) was used for determining elemental composition.

Bioassay of tribenuron-methyl against.eed. Firstly, maize plumule was used for comparing the effect of W-WSCA, H-WSCA and J-WSCA on bioactivity of tribenuron-methyl (T). Maize seeds were sown in agriperlite, watered and allowed to germinate in the dark at 26 ℃ for 2 days. The germinated seeds were laid in glass beaker with sterilized sand in 3cm high and covered by the sand in 3cm high again. Then the beakers were saturated with 1 μ g/ml of T without or with 5 μ g/ml of W-WSCA, H-WSCA and J-WSCA. Each treatment was repeated for three beakers. The weeds were grown in a greenhouse with a photoperiod of 16 h (22-25 ℃ in the light, 16-18 ℃ in the dark). After a week, the length of plumules was measure. Secondly, *Brassia campestri* was planted with pot culture in greenhouse in order to dose-response assays and index of relative toxicity. When the weed developed one leaf, herbicides were applied with spraying. Based on the prepared test, the tribenuron-methyl concentrations of 0.30, 0.90, 2.70, 8.40, 24.30, 72.90 g a.i./hm^2 were used. The concentrations of W-WSCA and J-WSCA were 10 g/h hm^2. The fresh weight of plant above land was measured at 14 days after herbicides were applied three replications. The fresh weight loss ratio indicated the activity of T, T-W-WSCA and T-J-WSCA.

Field trials of T against weed in field of wheat. The field trials of T, T-W-WSCA and T-J-WSCA against weed in field of wheat were carried out in Taiyuan, Shanxi province on Apr. 23, 2000. The concentration of T was 2 g/hm^2 in all tests. The concentration of WSCA were 18.7 and 187g/hm^2, and the The test area was 30 m^2 in replication for 4 times with random arrangement. The fresh weight of weed was surveyed after 20th day. Duncan's test was used for statistical analysis.

Results and discussion

The elemental analysis and properties of WSCA were listed in Table 1 and Table 2. The highest content of phenolic hydroxyl was found in W-WSCA among the three kinds of WSCA, while the most carboxyl and HA in J-WSCA. WSCA can bond with Fe^{3+}, Ca^{2+} and Mg^{2+} because of its good metal complexer and prevent coagulation emerged. Coag. value means the capacity of WSCA against electrolyte. The capacity of WSCA obtained by oxidized degradation (W- and H-WSCA) is about 60 times as large as that existing in coal (J-WSCA).

Maize plumule was used for comparing the adjuvant effect of W-WSCA, H-WSCA and J-WSCA on bioactivity of tribenuron-methyl (T). The shorter the length of plumule was, the stronger the bioactivity of herbicide was. The result was shown in Fig 2. WSCA

can enhance the bioactivity of T. And WSCAs newly formed through oxidation-degradation of coal were better than that existed in coal. W-WSCA was the best.

Table 3 listed the parameter of dose-response assays of T, T-W-WSCA and T-J-WSCA. The results of bioassay on *Brassia campestri* showed that W-WSCA and J-WSCA can enhance the inhibitory action of T on plant growth. ED_{50} (the concentration of herbicide when the death ratio of weed is 50%) of T, T-W-WSCA and T-J-WSCA was 1.20, 0.90 and 1.05 g a.i./hm^2. Using T as standard, index of relative toxicity of T-W-WSCA and T-J-WSCA was 133.3 and 115.4, respectively. From Table 4 it was seen that the index of relative toxicity was increased with increasing effective dose of T in the mixtures. The index of relative toxicity of the mixture of WSCA with T is more remarkable at ED_{70} than that ED_{50}, which further indicates the adjuvant effect of WSCA on T.

The field trials of T, T-W-WSCA and T-J-WSCA against weed in field wheat also proved the adjuvant effect of WSCA on T. The results were listed in Table 5. The effectiveness differed with different weeds. For *Lepiaium* and *Amaranthus retroflexus L*, the effectiveness of T with WSCAs were 2 times than that of T without WSCA. For other weed, WSCAs can raise 20% of T effectiveness.

Table1 Elemental analysis of W-WSCA and J-WSCA

Samples	Elemental analysis /W % daf					Functional Group$_{daf}$	
	C	H	O	N	S	OH_{ph}	COOH
W-WSCA	60.15	3.65	28.52	2.38	3.38	2.96	3.46
H-WSCA	60.91	3.62	29.87	3.04	0.59	1.92	4.25
J-WSCA	50.01	3.14	44.57	0.91	0.87	1.52	8.96

Table2 Properties of W-WSCA and J-WSCA

Samples	M_{ad} %	A_d %	HA_{daf} %	pH	Coag. value mmoll$^-$
W-WSCA	8.71	33.33	58.12	4.0	<36
H-WSCA	9.56	41.26	39.25	3.5	<36
J-WSCA	13.2	5.50	94.50	1.0	0.6

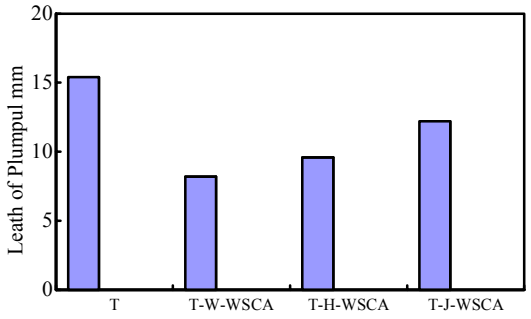

Figure 2 Effect of WSCA on the restraint of T on maize plumule

Table 3 Parameters of T, T—W-WSCA and T—J-WSCA

herbicide	Regression line y=a+bx	ED_{50} g/h hm^2	r	Index of relative toxicity
T	y=5.61+0.56x	1.2	0.9958	100
T—W-WSCA	y=5.88+0.72x	0.9	0.9942	133.3
T—J-WSCA	y=5.77+0.65x	1.05	0.9975	115.4

Table 4 Effective dose of T, T—W-WSCA and T—J-WSCA in dose-response assays

ED_p	Effective dose g/hm^2		
	T	T—W-WSCA	T—J-WSCA
ED_{30}	0.15	0.15	0.15
ED_{50}	1.20	0.90	1.05
ED_{70}	10.20	4.82	6.30

Conclusion

WSCA can enhance the biological activity of glyphosate, and the adjuvant effect was significant. The action of newly formed W- and H-WSCA was better than that of J-WSCA originally existed in coal. Moreover, the cost was reduced because W-WSCA and H-WSCA were the raw product, while J-WSCA was the purified product.

Table 5 Adjuvant effect of WSCA on G against weed in orchard with class

herbicide	Effectiveness at 20th day after herbicide applied											
	Aretisia		Chenopoaium Serotinium		Bothirospeimum chinense bge		Lepiaium		Amaranthus retroflexus L.		Convolvulus arvensis	
T	69.7 b	B	54.7 a	AB	68.4 b	B	44.9 b	B	43.0 b	B	73.9 c	B
T—W-WSCA$_1$	86.4 a	A	71.7 a	A	82.0 a	A	88.9 a	A	83.3 a b	A	92.2 ab	A
T—W-WSCA$_2$	94.6 a	A	87.9 a	A	85.7 a	A	95.8 a	A	92.7 a	A	96.9 a	A
T—J-WSCA$_1$	88.2 a	A	68.8 a	A	80.8 a	A	91.8 a	A	87.9 a	A	89.5 b	A
T—J-WSCA$_2$	95.4 a	A	80.6 a	A	88.9 a	A	95.3 a	A	95.3 a	A	98.4 a	A

W-WSCA$_1$ and W-WSCA$_2$ means the content of WSCA were 18.7, 187 g/hm^2, J-WSCA$_1$and J-WSCA$_2$ 18.7 and 187 g/hm^2.

Reference

1. Tang, C.C., Pesticide Chemistry, Nankai University Press, Tianjing, China, 1998.
2. Kuckuk, R., Hill, W., Nolte, J., Pestic. Sci., 1997, 51, p450-454.
3. Almendros, G. European Journal of Soil Science, 1995, 46, p287-301.
4. Chlou, C.T., Malcolm, R.L., Brlnton, T.I. Environ. Scl. Technol. 1986, 20, p502~508.
5. Cary, G.A., Mcmahon, J.A., Kuc, W.J., Environmental Toxicology and Chemistry, 1987, 6, p469~474.
6. Day, K.E ., Environmental Toxicology and Chemistry, 1987, 10, p91-101.
7. Senesi, N., The Science of the Total Environment, 1992, 123/124: 63~67.
8. Graham, A.G., Amar, Nath N.S., United States Patent 4062855, 1977.
9. Rehberg, B.E., Hall, W.L., United States Patent 5174804, 1992.
10. Li, S.X., Zhang, C.F., Li, B.Q., China States 99117700.2, 1999.
11. Li, S.X., Zhang, C.F., Li, B.Q., China States 99124922.4, 1999.
12. Schnitzer, M., Khan, S.U., Humic Substances in the Environment, MARCEL DEKKER. INC. press, New York, US, 1972.

OXIDATION OF BITUMINOUS COAL IN ALKALINE SOLUTION WITH FATTY ACID AS PROMOTER

Zhang Qiu-min Guan Jun Zhao Shu-chang Guo Shu-cai

Coal chemical institute of Dalian University
of Technology, Dalian 116012 China

Introduction

Coal has several positive attributes when considered as a feedstock for aromatic chemicals, specialty chemicals, and carbon-based materials. Substantial progress in advanced polymer materials, incorporating aromatic and polyaromatic units in their main chains, has created new opportunities for developing value-added or specialty organic chemicals from coal.

Coal oxidation in alkaline solution can directly obtain a mixture so-called coal acid (CA), aromatic carboxylic acid are mainly contained. Among them the major part is benzene ploycarboxylic acids, which are quite useful. But the mixtures are too complex to be completely separated. The recent researches indicated that selective decarboxylation and isomerization can extend the utilization of coal acid by converting them into value-added chemicals such as terephthalic acid, benzene tetracarboxylic acid and simple mixture of benzene dicarboxylic acid ect.

Based on this point of view a new method including oxidation of bituminous coal followed by coal acids isomerization to producing Terephthalic acid. The work was focused on the influence of fatty acid on coal oxidation by oxygen and alkaline solution. Based on it, other reaction conditions are also investigated.

Experimental

Two coals (DT coal and CT coal), which have great different in coalification, had been used in this work. Table 1 shows the analysis result.

Table 1. Analysis of Samples

	Proximate analytical %			Ultimate analytical % (daf)			
Sample	Mad	Aad	Vdaf	C	H	N	S
DT COAL	3.52	3.29	30.61	84.06	4.65	0.78	0.41
CT COAL	1.72	10.65	13.09	90.56	3.99	1.39	1.37

Coal is oxidized by oxygen and alkaline solution in an autoclave by adding fatty acid as promoter. Discharge materiel after cooling, separate coal cinder (unreacted coal and mineral matter) by filtration. Filter liquor is acidized to PH=3 by concentrated sulphuric acid, separate deposition (humic acids) by another filtration. Then the filter liquor is acidized to PH=1.5, thus water soluble acids dissociated. Coal acid can be obtained after except the solution by butanone and desiccate butanone by vacuum drying. The colors of coal acids are from yellow to brown.

Coal acids were analyzed both qualitatively and quantificationally by gas chromatograph after esterification by diazomethane.

Results and discussion

Promoter. The activity of acetic acid and propanoic acid are appraised under fixed oxidation conditions of temperature 270 °C, reaction time 2h, ratio of alkali to coal 3 to 1, CO_2 initial pressure 6.0Mpa, water to coal ratio 6 to 1, in K_2CO_3 solution, aiming at the yield of CA. Results are shown in **Figure 1.**

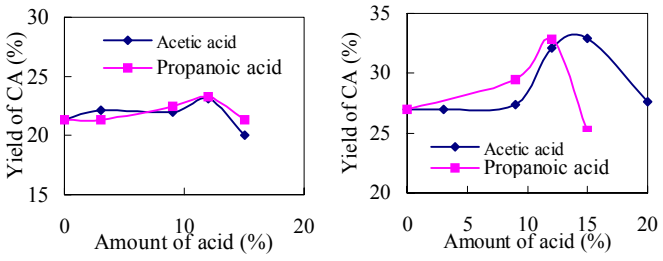

A---DT COAL B---CT COAL

Figure 1. Yield of CA from different amount of promoter by coal oxidation in K_2CO_3 solution

The result indicates that both acetic acid and propanoic acid can promote coal oxidation a lot but the activities of the two promoter and the influences on different coal are a little difference. The optimum amount of the is about 12%, and the yield of CA for DT coal increased from 21.3% to 23.1% with acetic acid, and to 23.3% with propanoic acid, compared to that without promoter.

For CT coal, the yield of CA increased from 27.0% to 32.95% by adding acetic acid, and to 32.8% by propanoic acid, which is a 22% increase relatively.

For compare the activities in different alkaline solution, an oxidation experiment has done with DT coal and CT coal adding acetic acid as promoter in KOH solution. The conditions are similar except for ratio of alkali to coal (2 to 1) and ratio of water to coal (5 to 1). Figure 2 shows the results.

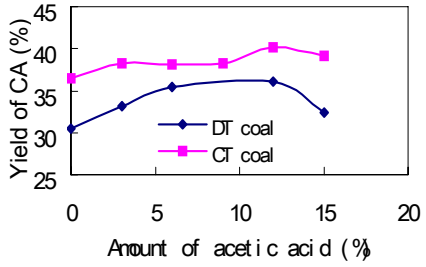

Figure 2. Yield of CA from different amount of acetic acid by coal oxidation in KOH solution

As shown in **Figure 2**,the influences of amount of acetic acid to the yield of CA are similar to those in K_2CO_3. The optimum amounts of the promoter for two coals are also about 12%. For DT coal oxidation under optimum conditions, the yield of CA grew from 30.5% (daf) to 36.1% (daf), which is a 18.5% increase relatively. For CT coal oxidation, the yield of CA grew from 36.5% (daf) to 40.0% (daf) , which is a 9.9% increase relatively.

Reaction temperature. Since the activities of the two promoters are about the same, only acetic acid used as the promoter here.

Figure 3 shows the influences of reaction temperature to the yield of CA under the conditions motioned above, except that the ratio of alkali to coal is 4 to 1 and the amount of acetic acid is 12%.

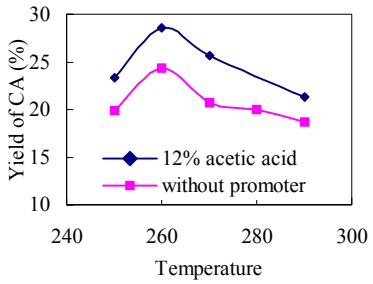

Figure 3 Change in yield of CA through the temperature

The yield of CA rose sharply with temperature grew from 250℃ to 260℃, and then declined. The optimum temperatures are 260℃. Under optimum temperatures, the yield of CA grew from 23.33% (daf) without acetic acid to 28.6% (daf) with 12% acetic acid as promoter, which is an 18% increase relatively. The yields of CA with promoter are higher in the range 250～290 ℃.

Ratio of alkali to coal .Figure 4 shows the influences of ratio of alkali to coal to the yield of CA under the conditions motioned above, in K_2CO_3 solution.

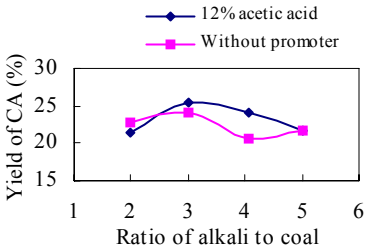

Figure 4. Change in yield of CA through the ratio of alkali to coal

Yield of CA through the ratio of alkali to coal first rose, via maximum, and then declined. With or without promoter, the optimum ratios of alkali to coal are 3～4. The yields of CA with promoter added are higher than those blank one in the whole range.

Reaction time. Figure 5 shows the influences of reaction time to the yield of CA under the conditions motioned above, except that the ratio of alkali to coal is 4 to 1 and the amount of acetic acid is 12%.

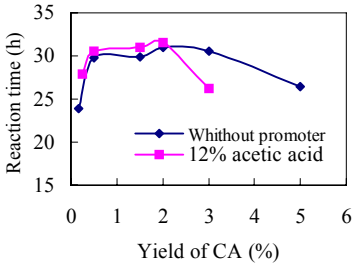

Figure 5. Change in yield of CA through the reaction time

The yield of CA grew sharply before half an hour, and then fixed as time goes through. With or without promoter the maximum yield of CA are similar. The yield of CA declined after 5h without promoter and declined after 3h with promoter, this shows promoter can promote the oxidation.

Composition of coal acids. This paper merely analyzed composition of coal acids with chromatogram under optimum amount of acetic acid as promoter. BPCA in coal acids are qualitatively and quantitatively analyzed, which are the calculations of composition of coal acids and yields of BPCA based on, as shown in table 2.

Table 2. Composition of Coal Acids

compositition		DT COAL (added in acetic acid)		CT COAL(added in acetic acid)	
		0%	12%	0%	12%
Yield of CA %(daf)		24.33	28.67	36.54	40.14
Benzoic acid		0.48	0.73	0.14	1.16
Benzene dicarboxylic acid	1,2	5.79	9.44	11.93	17.34
	1,4	—	—	1.32	1.81
	1,3	—	—	0.38	2.11
Benzene tricarboxylic acid	1,2,3	4.56	6.79	6.13	10.96
	1,2,4	6.28	8.71	10.56	12.66
	1,3,5	0.69	5.28	0.30	0.26
Benzene tetracarboxylic acid	1,2,3,4	8.03	14.23	11.09	17.85
	1,2,4,5	4.77	6.52	6.18	7.42
	1,2,3,5	3.10	4.63	3.67	4.40
Benzene pentacarboxylic acid		—	—	7.39	9.93
Benzene hexacarboxylic acid		—	—	1.54	1.53
Total		33.7	56.89	60.62	87.68
Yield of BPCA % (daf)		8.20	16.31	22.13	35.18

* in K_2CO_3 medium **in KOH medium

Table 2 shows composition of coal acids and yields of BPCA from DT COAL oxidation in K_2CO_3 medium and CT COAL oxidation in KOH medium. DT COAL oxidation compared with no promoter, the BPCA content of CA increased enormously by adding 12% acetic acid in rose from 33.7% to 56.89%, which is a 68.8% increase relatively. The yields of BPCA to coals grew from 8.2% to 16.31%, which is a 98.8% increase relatively. CT COAL oxidation compared with no promoter, the BPCA content of CA increased also enormously by adding 12% acetic acid in rose from 60.6% to 87.8%, which is a 44.7% increase relatively. The yields of BPCA to coals grew from 22.1% to 35.2%, which is about 60% increase relatively.

The effect of adding acetic acid at the amount of 12% on coal oxidation is not only it can improve the yield of CA but also it can improve the content of BPCA in CA sharply, which lead to the yields of BPCA to coal increased. This further evidenced that the promoter has directional function to coal oxidation.

Acknowledgment

This work was supported by National Natural Science Foundation of China (29806003)

Reference

1. Song, C.S.; Schobert, H.H., *Fuel Proc. Technol.,* 1993. 34: P. 157-196.
2. Schobert, H.H., Song, C.S., *Fuel*, 2002. 81(1): P 15-32.
3. Salbut,P.D., Mozliwosci, *Przem. Chem.,* 1986. 65(1): P 23-35
4. Zhao shu-chang, Deng Yizhao, *Journal of Dalian University of Technology,* 1994. 34(6): P 682

PREPARATION OF TEREPHTHALIC ACID BY COAL ACIDS ISOMERIZATION

Zhang Qiu-min Guan Jun Zhao Shu-chang Guo Shu-cai

Coal chemical institute of Dalian University of Technology, Dalian 116012 China

Introduction

Coal may become more important both as an energy source and as the source of organic chemical feedstock in the 21st century. Coal has several positive attributes when considered as a feedstock for aromatic chemicals, specialty chemicals, and carbon-based materials. Substantial progress in advanced polymer materials, incorporating aromatic and polyaromatic units in their main chains, has created new opportunities for developing value-added or specialty organic chemicals from coal.

Coal oxidation in alkaline solution can directly obtain a mixture so-called coal acid (CA), aromatic carboxylic acid are mainly contained. Among them the major part is benzene ploycarboxylic acids, which are quite useful. But the mixtures are too complex to be completely separated. The recent researches indicated that selective decarboxylation and isomerization can extend the utilization of coal acid by converting them into value-added chemicals such as terephthalic acid, benzene tetracarboxylic acid and simple mixture of benzene dicarboxylic acid ect.

Based on this point of view this paper provides a new method of non-fuel uses of coal that is Oxidation of Bituminous Coal and Preparation of Terephthalic Acid by Coal Acids Isomerization. Based on it, other reaction conditions are also investigated. The influences of temperature, initial pressure of CO_2, reaction time and amount of catalyst to the yield of TPA are mainly investigated in iosmerization. And the optimum conditions are found out. High-activated cadmium salt is used as catalyst. Coal acids are prepared into kali salt before isomerization.

Experimental

Coal acids for isomerization were the mixture of oxidation product obtained. Using KOH to prepare kali salt of CA and using $CdCO_3$ as catalyst. **Table 1** shows the analyses of mixed coal acids by chromatogram.

Table 1. Analyses of Mixed Coal acids by Chromatogram

Composition		
Benzoic acid		-
Benzene dicarboxylic acid	1,2	9.11
	1,4	-
	1,3	0.8
Benzene tricarboxylic acid	1,2,3	0.98
	1,2,4	7.16
	1,3,5	9.45
Benzene tetracarboxylic acid	1,2,3,4	13.00
	1,2,4,5	6.75
	1,2,3,5	3.98
Benzene pentacarboxylic acid		1.64
Benzene hexacarboxylic acid		10.86
Total		63.73

Use a micro reactor (25ml) isomerizate kali salt of CA, with $CdCO_3$ as catalyst and in CO_2. The product is so-called black powder. Crude TPA can be obtained after dissolve by water, filtration and acidification.

Put the micro reactor in after sand bath stove was adjusted into an appropriate temperature. The temperature of reactor would reach the reaction temperature with in 10 min.

Figure 1 shows the equipment.

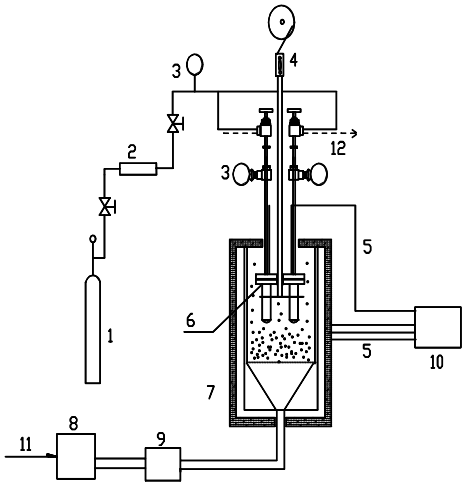

1. CO_2 cylinder 2. Drying tube 3. Pressure gage
4. Bracket 5. Thermoelement 6. Reactor
7. Sand bath stove 8. Air compressor 9.Preheater
10. Control system 11. Air 12. CO_2

Figure 1. The equipment for isomerizatiom

Coal acids and TPA were analyzed by gas chromatogram after esterification by diazomethane. The purity of TPA was analyses by titration at same time.

Results and discussion

Catalyst. The results obtained with fiffrent amount of catalyst ($CdCO_3$) are shown in Figure 2, 470℃, 2h, and CO_2 initial pressure 1Mpa，has investigated.

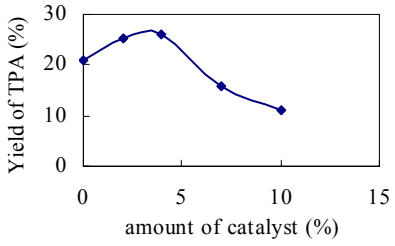

Figure 2. Influence of amount of catalyst to the yield of TPA

As shown in **Figure 2**, the yield of TPA is 20.79% without catalyst $CdCO_3$ at 470℃. As the amount of $CdCO_3$ grows, the yields of TPA grew and reached the maximum yield at 4%. This expresses the beneficial function of isomerization with catalyst. The yield of TPA declined when the amount of catalyst exceeded 4%, which indicates large amount of catalyst would restrain isomerization. Therefore the optimum amount of catalyst is 4%, the optimum yield of TPA is 23.5%.

Initial pressure of CO_2. Figure 3 shows the influence of initial pressure of CO_2 to the yield of TPA with $CdCO_3$ as catalyst(7%), 470℃, 2h .

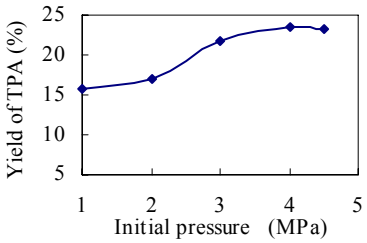

Figure 3. Influence of initial pressure of CO_2 to the yield of TPA

As shown in **Figure 3**, the yield of TPA grew sharply before 3.0MPa,then grew slowly during 3.0-4.0MPa, and then fixed after 4.0MPa. Increase of initial pressure of CO_2 not only added the opportunities of CO_2 molecule impact, but also benefit to carboxylation reaction. Therefore the appropriate pressure of CO_2 is necessary, 4.0MPa is properly.

Temperature. Temperature is the most important factor. Isomerizations proceeded within the scope 410-470℃. To compare the experiment, isomerizations with benzoic acid adding in proceeded at the same time. Figure 4 shows the result.

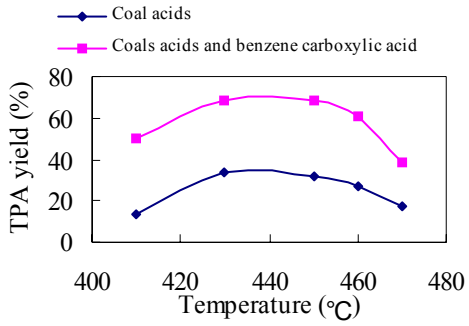

Figure 4 Influence of temperature to the yield of TPA

Figure 4 shows that without adding benzoic acid the yield of TPA grew as temperature rose, maximum yield of TPA occurs at 430℃-450℃, and then declined. Isomerization is incomplete at low temperature. When temperature is higher than 450℃, polymerization and carbonization occur seriously, the color of production darken, then led to the declination of yield. The optimum temperature(about 450℃) of isomerizating by kali salt of coal acid and kali salt of benzoic acid are similar to that of kali salt of coal acid isomerization only, except that the yield of TPA is much higher. The yield of crude TPA rose from 34.10% to 68.58% by adding kali salt of benzoic acid. The yield of TPA to CA is up to 70% deducting the theoretical yield of BA dispropornation, which is two times of CA isomerization only. It is advisable to add benzoic acid in when the coal acid contains too much high-level benzene polycarboxylic acids.

Reaction time. Figure 4 shows the influence of reaction time to the yield of TPA with $CdCO_3$ as catalyst(7%), 470℃, 2h .

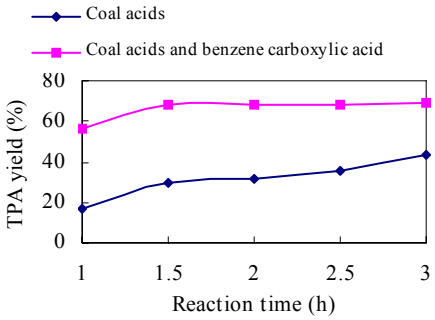

Figure 5 Influence of reaction time to the yield of TPA

The yield of TPA grew as reaction time less than 1.5h and increased a little after 1.5h, as **Figure 5** shows. Isomerizitions of kali salt CA are fundamentally completed therefore the yield of TPA no longer increased. It is confirmed that 2h is the optimum reaction time. The yield of crude TPA also rose more than 100% by adding kali salt of benzoic acid.

Product purification

Crude TPA which purity is about 90% can be obtained after dissolve by water, filtration and acidification. The purity can be further improved by hot water scrubbing and activated carbon discoloring, reaching 99.37% after once and 99.71 after twice.

Conclusion

1.The better conditions of kali salt of coal acid isomerizating are temperature 430-450℃, initial pressure of CO_2, 4.0Mpa, content of catalyst 4%, reaction time 2h. The optimum conditions of isomerizating by kali salt of coal acid and kali salt of benzoic acid are similar to that of kali salt of coal acid isomerization only.

2.The yield of crude TPA to CA is about 34% in case of coal acid isomerizating. It equals to 75% of the theoretical yield to BPCA.

3.The yield of crude TPA is up to 68% when kali salt of coal acid and salt of benzoic acid isomerizating under the best conditions. The yield of TPA to CA is up to 70% deducting the theoretical yield of BA dispropornation, which is two times of CA isomerization only. It is advisable to add benzoic acid in when the coal acid contains too much high-level benzene polycarboxylic acids.

4.The TPA purity can be further improved by refining crude TPA, reaching 99%.

Acknowledgment

This work was supported by National Natural Science Foundation of China (29806003)

Reference

1. Song, C.S.; Schobert, H.H., *Fuel Proc. Technol.,* 1993. 34: P. 157-196.
2. Schobert, H.H., Song, C.S., *Fuel*, 2002. 81(1): P 15-32.
3. Salbut,P.D., Mozliwosci, *Przem. Chem.,* 1986. 65(1): P 23-35
4. Zhao shu-chang, Deng Yizhao, *Journal of Dalian University of Technology,* 1994. 34(6): P 682